UNIVERSITÀ POLITECNICA DELLE MARCHE

DIPARTIMENTO SCIENZE DELLA VITA E DELL'AMBIENTE

**Corso di Laurea Magistrale
Biologia Marina**

IMPATTO DELLE ATTIVITA' MINERARIE IN AMBIENTE PROFONDO SU VIRUS, PROCARIOTI E MICROEUCARIOTI BENTONICI E SUI CICLI BIOGEOCHIMICI

IMPACT OF DEEP-SEA MINING ON BENTHIC VIRUSES, PROKARYOTES, MICROEUKARYOTES AND ON BIOGEOCHEMICAL CYCLES

Tesi di Laurea Magistrale di:

Masha Prosperi

Relatore
Chiar.mo Prof.

Roberto Danovaro

Correlatore:

Antonio Dell'Anno

Sessione Straordinaria Febbraio 2023

Anno Accademico 2021/2022

Contents

Riassunto

Il rapido aumento della popolazione globale e lo sviluppo socio-economico hanno portato ad un incremento nella domanda di risorse minerarie.

Nelle profondità oceaniche sono custoditi metalli di elevato interesse economico come Mn, Cu e Co sottoforma di concrezioni minerarie chiamate "noduli polimetallici". I noduli hanno un enorme potenziale per lo sviluppo commerciale (es. batterie ricaricabili); tuttavia va considerato anche il ruolo che queste strutture rivestono per gli organismi sessili e per il mantenimento dell'eterogeneità di questi habitat.

Una delle aree oceaniche più ricche di noduli è localizzata nel Pacifico equatoriale, tra 4000-5500 metri di profondità, ed è conosciuta come "Clarion-Clipperton Zone" (CCZ) caratterizzata da un'estensione di 5000 km^2 con una densità media di noduli di 15 kg/m^2.

Questa tesi è stata condotta nell'ambito di un progetto internazionale del "Joint Programming Initiative Healthy and Productive Seas and Oceans (JPI-Oceans)" nella CCZ dove è stata simulata una attività estrattiva di noduli polimetallici attraverso il primo prototipo industriale, chiamato Patania II.

Lo scopo della presente tesi è quello di investigare, attraverso diverse analisi, l'impatto che future attività di mining potrebbero avere sullo stato trofico e sulle componenti microbiche bentoniche.

In particolare, sono state svolte le seguenti analisi: i) quantità e composizione della materia organica sedimentata (in termini di proteine, carboidrati, lipidi e pigmenti), ii) abbondanza e biomassa procariotica nel primo centimetro di sedimento, iii) attività enzimatiche extracellulari e turnover-time nei sedimenti, iv) abbondanza e produzione virale nel primo centimetro di sedimento, v) diversità microeucariotica.

L'impatto del collettore è stato testato su due aree delle quali una in concessione alla Germania e l'altra al Belgio. Prima dell'impatto le due aree mostravano differenze significative nel contenuto e nella composizione della sostanza organica sedimentata, nelle attività enzimatiche extracellulari e nelle comunità microbiche. Tali risultati sono supportati da studi precedenti i quali hanno evidenziato che la CCZ è soggetta a differenze spaziali nel flusso di carbonio al fondo in cui l'area tedesca è soggetta ad un maggiore apporto rispetto a quella belga.

In seguito all'azione di Patania II le due aree mostrano una diminuzione nel contenuto della materia organica in tutti gli strati analizzati, con una diminuzione più severa nel contenuto di fitopigmenti. Questi risultati, dunque, indicano che l'effetto meccanico delle attività minerarie condotte da Patania II portano ad un "impoverimento trofico" non solo nello strato più superficiale del sedimento ma anche fino a 5 cm di profondità.

Oltre a ciò, è stata osservata una diminuzione delle attività enzimatiche extracellulari e dell'abbondanza dei procarioti bentonici a seguito dell'impatto di Patania. La componente dei microeucarioti bentonici mostrava anch'essa delle variazioni nella composizione dei taxa dominanti prima e dopo l'impatto. Questi risultati supportano l'ipotesi secondo la quale l'impatto dato dal passaggio di Patania II è quello di causare uno shift di taxa microeucarioti probabilmente connesso alla ri-sospensione dei sedimenti e/o alla mortalità di alcuni di essi.

In conclusione, i risultati di questa tesi evidenziano che l'estrazione mineraria da ambienti profondi può determinare importanti cambiamenti su componenti bentoniche di grande rilevanza nella trofodinamica e nei cicli biogeochimici di tali ecosistemi, con potenziali effetti a cascata sul loro funzionamento complessivo.

Preface

The rapidly increasing global populations and socio-economic development have resulted in rising demand for natural resources.

There are many plans for harvesting natural resources from the ocean floor, especially rare metals and minerals; high-capacity and high-quality ore deposits are becoming arduous to unearth, so the search expands to the deep seabed as an alternative for low-grade mining (Filho et al., 2021).

The deep-seabed, especially the abyssal plains (seafloor between 4000 and 6000 m water depth), have been relatively untouched by anthropogenic impacts due to their extreme depths and distance from continents (Ramírez-Llodrà et al., 2011).

There are metals of economic interest such as manganese (20-30%), nickel (1.25-1.5%), copper (1-1.4%) and cobalt (0.2-0.25%) and other rare metals that have also tremendous potential for commercial development (Marine Mineral Resources; ISA); in fact, these metals are becoming important for modern life, since they are used in making electronics like rechargeable batteries and touch screens, among other things.

These metals, in different concentrations, occur in concretions called "polymetallic nodules" found in various deep-sea ocean regions, including the

deep Pacific and Indian Oceans (Figure A), with a predominantly discoidal
shape and a size range of 2–8 cm in these regions (Kuhn et al., 2017).
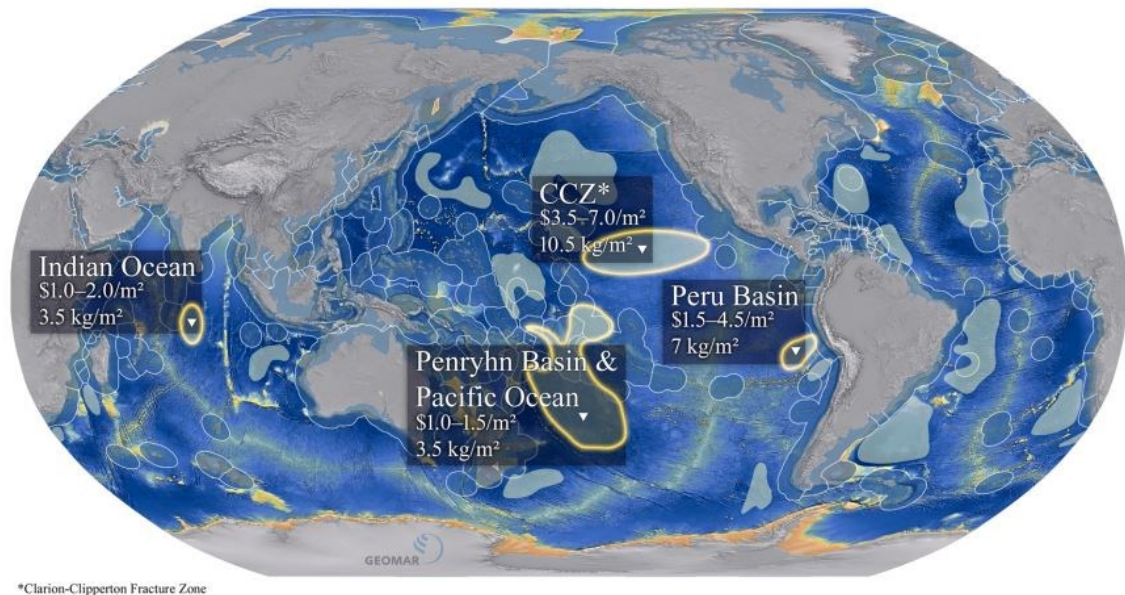

Figure A: Global occurrences of seabed manganese nodules. Cash values refer to the mean value (2015-US$ per m^2) of the years 1970 to 2015; estimated according to the methodology and data published by Volkmann et al. (2018)
Image credit - GEOMAR

Nodules provide the rare commodity of hard substrate in the abyss, they form
deposits within the first 10 cm of the deep-sea sediment, they are fundamental
for the heterogeneity of these habitat and deep-seabed mining targets these
mineral-rich nodules and will likely modify the consumer-resource (trophic)
and substrate-providing (non-trophic) interactions within the abyssal food
web (Stratmann et al., 2021).

One of the nodule-richest areas in the global ocean is localized in the Pacific
Ocean, between ~4,000 - 5,500 meter in depth, and is known as the Clarion-

Clipperton Zone (CCZ). This area covers 5,000 kilometres and harbours an average nodule density of 15 kg m-^{2} (Hein and Petersen, 2020).

This thesis is part of the project conducted within the frame "Joint Programming Initiative Healthy and Productive Seas and Oceans (JPI-Oceans)" conducted in the CCZ in 2015-2022. The JPI-O project aims at increasing "the efficiency and the impact of research and innovation for sustainably healthy and productive seas and oceans" (Jpi-oceans.eu). The studies based on the "Ecological aspects of deep-sea mining" began in 2015 up to 2017 with pilot actions based on assessing the ecological impacts which could arise from commercial mining activities in the deep-sea. The second phase of the project began on August 2018 and finish on February 2022 and was based on the "Environmental impacts and risks of deep-sea mining" and included two cruises: SO268 and MANGAN 2021. This second phase was developed toward three major research interests concerning deep-sea mining: (1) the larger scale environmental impact caused by the suspended sediment plume, (2) the regional connectivity of species and the biodiversity of biological assemblages and their resilience to impacts, and (3) the integrated effects on ecosystem functions, such as the benthic food-web and biogeochemical processes (JPIO Mining Impact (geomar.de)).

Here we analyse samples collected during the oceanographic cruise "MANGAN 2021" focusing on the effects of deep-sea mining on ecosystem functioning.

While the first project phase could investigate only experimental and/or rather small-scale disturbances of the seafloor, in the second phase a comprehensive monitoring program was devoted to the industrial test of the prototype nodule collector system named Patania II.

The aim of the present thesis is to better understand through different analyses the effectiveness of the impact on biodiversity and biogeochemical cycles in benthic deep-sea ecosystems. In particular, will be analysed the mining impact in terms of:

- Status of trophic system (Organic Matter) and biogeochemical cycles (hydrolyzation rate) in the first 5 cm of the core's horizon

- Virus-Prokaryotic relations after the impact

- Diversity and variability of microeukaryotes

- Spatial variability of the impact between the two different areas before and after impact.

To do this the following analyses has been performed:

- Sedimentary organic matter (OM) in quantity and composition

- Prokaryotic abundance and biomass in the 0-1 cm horizon

- Extracellular enzymatic activities and proteins turnover-time in the sediments

- Viral abundance and production in the 0-1 cm horizon

- Microeukaryotes biodiversity

The results in this work of thesis will increase our knowledge on the effects of Patania II in the deep-sea environment in terms of biodiversity and functioning on benthic deep-sea ecosystems in two different ways: the vertical impact from 0 to 5 cm and the horizontal spatial comparison of the two different areas considering the before and after impact, will be observed.

1. Introduction

Deep-sea ecosystem (>200 m below sea level) cover ~65% of the Earth's surface and ~95% of the ocean sea floor is covered by deep-sea sediments, which are the largest ecosystem on Earth that control global biogeochemical cycles (Danovaro et al.,2014; Canals et al.,2006). Deep-sea is one of the most fragile and less explored environments and it preserves a wide range of resources useful to human as oil, gas, fisheries and minerals. Increasing exploration and industrial exploitation of this vast and delicate environment raises global concerns about potential and cumulative ecological impacts, both for pelagic and benthonic ecosystems, caused by human activities that may act synergistically and could eventually cause regime shifts and alter deep-sea ocean life-support services, such as the biological pump or nutrient (Ramírez-Llodra et al., 2011; Snelgrove et al., 1997; Thurber et al., 2014).

Life in benthic deep-sea ecosystems is also largely constrained by the limited and episodic food supply from the water column (Danovaro et al., 2014); Molari et al., 2013).

Abyssal plains of all major oceans (~4000-6000 m water depth) harbour extensive fields of manganese nodules. These mineral aggregates occur as potato-shaped concretions consisting of manganese, nickel, copper, and cobalt

but also rare earth metals such as molybdenum, titanium and lithium (Kuhn et al., 2017).

The nodules consist of concentrically banded zones of micro-layers around a nucleus. They form by metal precipitation either from the ambient seawater (hydrogenetic) or from pore water in the sediments (diagenetic). They generally consist of a mixture of both hydrogenetic and diagenetic composition but in varying proportions (Kuhn et al., 2017).

Polymetallic nodule fields provide hard substrate for sessile organisms (Porifera, Antipatharia, Alcyonacea or Ascidiacea) on the abyssal seafloor and they are also essential for food-web integrity due to the complexity of the feeding interactions (Stratmann et al., 2021). They add a network of non-trophic interactions (non-consumptive relationships between taxa) among sessile organisms and their associated fauna, to the classical trophic interactions that are known for abyssal food webs (Stratmann et al., 2021)

Moreover, nodules of the eastern tropical Pacific and the central Indian Ocean are of special economic interest due to their high enrichment of metals (e.g., Hein and Koschinsky 2013).

The area with the largest contiguous occurrence of manganese nodules fields is the Clarion-Clipperton fracture Zone (CCZ), it is located in the Central Pacific just north of the equator between Hawaii and Mexico (Figure 1).
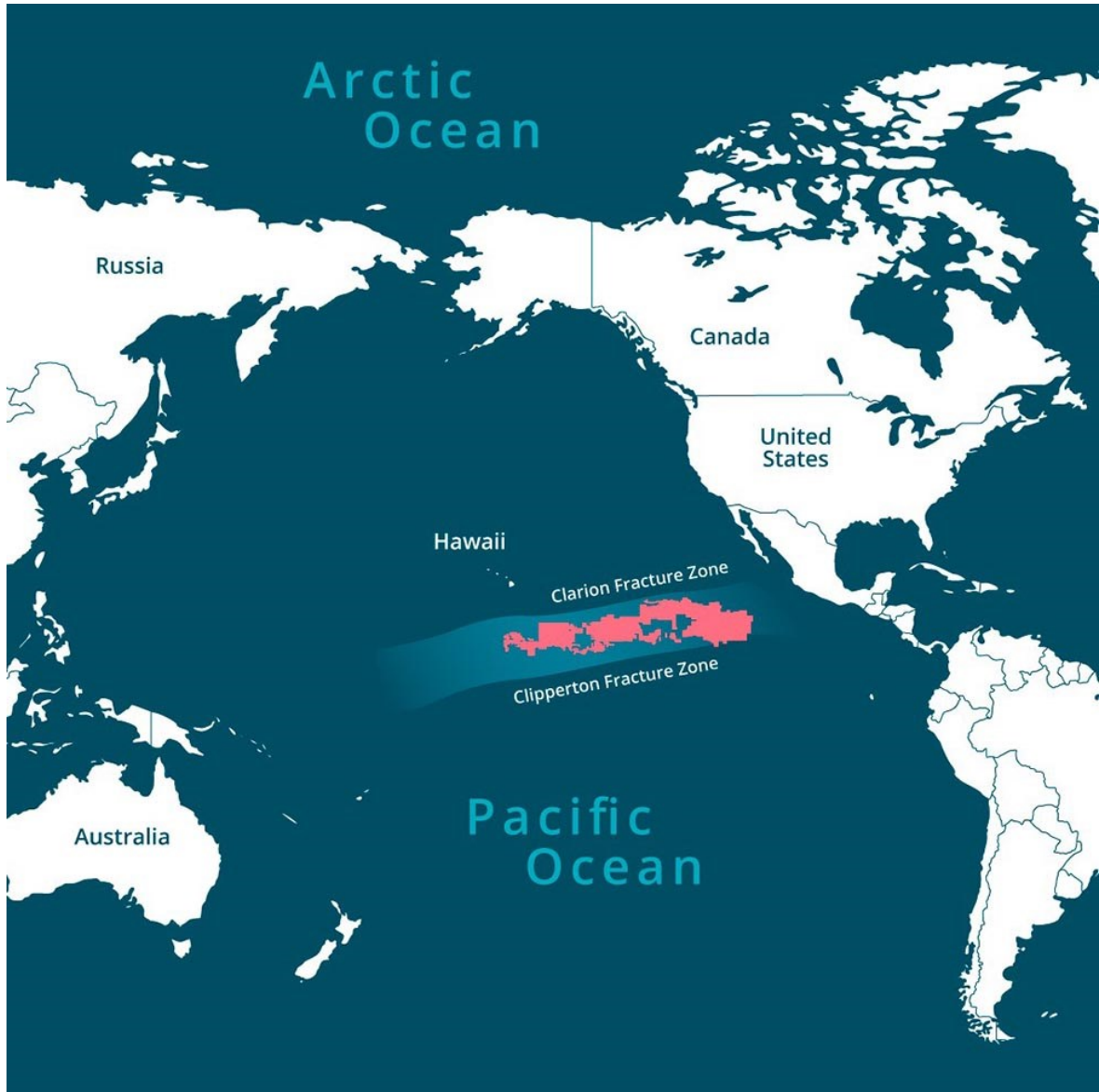
Figure 1: *the Clarion-Clipperton zone (CCZ) is one of the deepest point of the Pacific Ocean. Is an abyssal plain bound by the Clarion and the Clipperton Fractures with a length of ~5000 km (3100 miles). Image credit – Horizon (The EU research and innovation magazine)*

The growth rate of hydrogenetic layers is typically in the range of 1–5 mm per million years (Koschinsky and Hein, 2003 and references therein), whereas diagenetic layers grow considerably faster up to 250 mm per million years (von Stackelberg, 2000).

Diagenetic Mn flux rates are considerably higher than hydrogenetic Mn flux rates, which explains the high diagenetic growth rates (von Stackelberg 2000); altogether, Mn nodules grow with average rates of 10–20 mm per million years and usually have an age of several millions of years (Kuhn et al., 2017).

Apart from slight changes in the percentage typology of formation, the chemical composition of the nodules is relatively constant throughout the CCZ; however, polymanganese nodules are not equally distributed on the seafloor within the CCZ but occur in patches (Kuhn et al., 2017). Economically interesting "patches" can cover an area of several thousand square kilometres with nodules density ranging between 0 and ~30 kg/m^2 (wet nodules weight) with an average of 15 kg/m^2 (Beaudoin and Baker, 2013). Given the huge amounts of nodules in this area, the exploitation of these mineral aggregates could have a significant effect on the global industry (Kuhn et al., 2017).

The deep-sea mining industry is developing specialized underwater mining technology to harvest the remotely-located mineral sources (present in the Central Pacific Ocean in international water far from the coast) from thousands of square kilometres of seafloor. Mining will bring unavoidable loss of biodiversity because it will directly destroy life and seabed habitat (NOAA) and indirectly bring into suspension sediments plume, that are enriched in bioavailable metals, prokaryotic and microeukaryotic organisms, in large volumes of the water column (Van Dover et al., 2017).

The physical removal of nodules as hard-substrate habitats has severe consequences for the nodule-associated sessile fauna as well as the mobile fauna (Bluhm, 2001; Smith et al., 2008; Purser et al., 2016; Vanreusel et al., 2016), their removal in the CCZ resulted in a substantial and consistent reduction of 31% in the number of network links (Stratmann et al., 2021). With slow nodule growth rates of a few millimetres per million years (e.g., Halbach et al., 1988; Kuhn et al., 2017a), the deep-sea fauna may not recover for millions of years (Vanreusel et al., 2016; Jones et al., 2017; Gollner et al., 2017; Stratmann et al., 2018).

In addition to the removal of deep-sea fauna as well as seafloor habitats, the exploitation of nodules is associated with (1) the removal, mixing and re-suspension of the upper 4 sediment layers of the seafloor ; (2) the re-

deposition of material from the suspended sediment plume; and (3) potentially also the compaction of the surface sediments due to weight of the nodule collector (Thiel and Forschungsverband Tiefsee-Umweltschutz, 2001; Oebius et al., 2001; König et al., 2001; Grupe et al., 2001; Radziejewska, 2002; Khripounoff et al., 2006; Cronan et al., 2010; Paul et al., 2018; Gillard et al., 2019). Knowing that the first centimeters of bottom sediment are the richest part in nutrients (as they receive organic matter from the water column) and that the nodules we find there host sessile and vagile benthic organisms living on and in them, their removal can lead to a change in this heterogeneous, highly oligotrophic habitat modifying both the biogeochemical cycles and the food webs.

Considering that the CCZ is outside national jurisdiction, deep-sea mining in this region is regulated by the International Seabed Authority (ISA). Currently, contracts for mining exploration in the CCZ have been granted to 17 deep-sea mining contractors (ISA), with exploration areas covering approximately 1 million square kilometres and nine protected areas (Areas of Particular Environmental Interest; APEIs), which are currently protected from mining activities.

In 2021, four new APEIs areas were established for enhancing the effectiveness of the whole network (13 total APEIs) (Figure 2).

Each of these areas cover ~160,000 square kilometres and are located around the exploration license areas (ISA).

The APEIs were placed across the CCZ to protect and represent the full range of biodiversity and habitats in the region, including variations in nodule abundances, food availability, and seafloor topography (including the presence of seamounts) (NOAA).

Moreover, it is also important to consider restoration experiments conducted in this area: in 2021 Gollner et al. aims to test the feasibility of restoration measures after this test-mining activity in the deep-sea. They manufactured ceramic nodules made from clay and deployed these artificial hard substrates in the German and Belgian contract areas in the CCZ. Considering the slow natural recovery rates of deep-seafloor communities, the intention of this restoration action is to recover these artificial hard substrates about every five years, with an intended project duration of ~30 years.
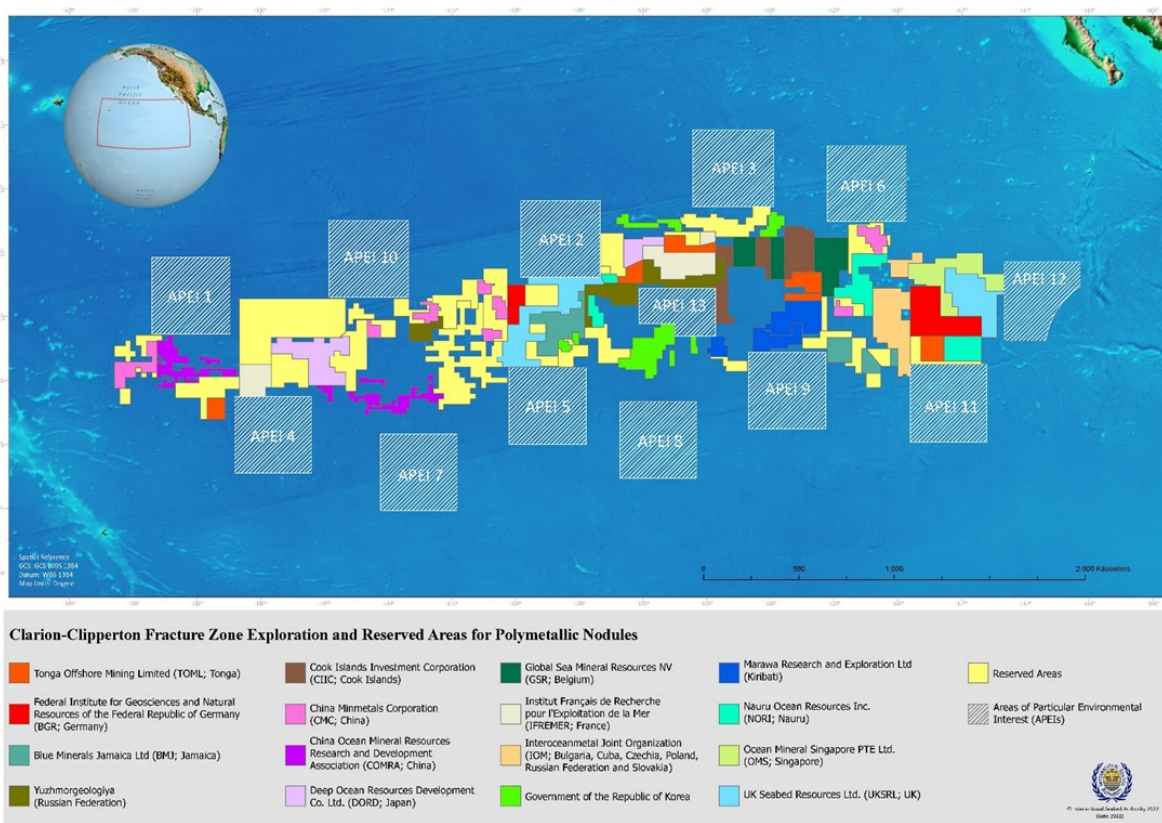
Figure 2: Sampling sites in various European contract areas for the exploration of manganese nodules within the Clarion–Clipperton Zone (CCZ).). The contract areas granted and governed by the International Seabed Authority (ISA; white areas) are surrounded by thirteen areas of particular environmental interest (APEIs), which are excluded from any mining activities (green shaded squares). Investigated sites in this work are located in the right German BGR area (red), and right Belgian GSR area (white).

Geographical data provided by the ISA.

In early April 2021, scientists from the BGR (Federal Institute for Geosciences and Natural Resources) and the European JPI Oceans project "MiningImpact" set off from San Diego (USA) on a 42-day expedition with the Norwegian ship "ISLAND PRIDE" to the Central Pacific. The aim was to carry out a detailed monitoring of the environmental impact of the first industrial mining tests that, in those same days, would have taken place in the belt between Hawaii and Mexico; the Belgian company "Global Sea Mineral Resources (GSR)" tested the collection of the metal-rich nodules from the seabed using a pre-prototype nodule collector Patania II (Figure 3).

The test was conducted at 4,500 metres depth and is the first of its kind worldwide.

König et al., 2001 have applied numerical modelling to study the

Figure 3: prototype collector (Patania II) used to test the collection of manganese nodules from the seabed. Source: GSR

consequences of the removal of the upper 10 cm of the sediments during mining activities in the DISCOL (*DISturbance and reCOLonization* experiments) area. They showed that the degradation of TOC (Total Organic Carbon) during aerobic respiration, denitrification and Mn reduction may be decreased for centuries, increasing the oxygen penetration depth (OPD).

These observations have recently been confirmed by Vonnahme et al., 2020, in which a decrease in biological processes in the first few centimetres of sediment was observed in the microbial communities 26 years after the impact.

Volz et al. 2020 suggest that mining techniques potentially used for the commercial exploitation of nodules in the CCZ will remove potentially ~7-10 cm of the surface sediments in order to minimize the impact on the geochemical system in the sediments.

This study aims at providing new insight into the potential impact of mineral exploitation activity on trophodynamics and biogeochemical cycles in benthic deep-sea ecosystems and on microeukaryotic communities inhabiting the CCZ.

To do so, sediments samples from the first 5 cm of the seafloor were collected before and after an *in-situ* simulation of deep-sea mining activities conducted with a hydraulic pre-prototype nodule collector called Patania II, in two

different areas of the Clarion-Clipperton Fracture Zone both before and after the mining impact.

In particular, this work of thesis investigated the potential impact of deep-sea mining on two licensed areas (the German and the Belgian Area) assessing the potential changes in: i) status of trophic system and ecosystem functioning; ii) relation between virus and prokaryotic after the impact; iii) microeukaryotes diversity and variability and iv) spatial variability of the impact between the German and the Belgian areas.

2. Materials and methods

2.1 Study areas, sampling design and samples collection

Sediments were collected in the framework JPI-O project between the 4th of April and the 17th of May 2021 during the oceanographic cruise "MANGAN 2021" in board the Island Pride IP21.

Samples were taken in 2 different sampling areas: the German and the Belgian licensed Area (Figure 4 and Figure 5) of the CCZ at a bottom depth of 4100 and 4500 m, respectively.

The sampling strategy for the two areas included a trial site, in which samples before (pre-impact) and after (post-impact) the mining experiment were collected. In each sampling area samples were collected with three independent deployments of the TV-guided multicore (TV-MUC) which allows collecting samples hermetically sealed.

Sediment samples were sliced in three horizons: 0-1 cm, 1-3 cm, 3-5 cm and were immediately stored at -20°C for the analyses of organic matter content and composition and extracellular enzymatic activities. Sub-samples from the top 1st cm were immediately processed for the analyses of viral production according to Dell'Anno et al., 2009 or stored at -20°C for the analyses of prokaryotic abundance and biomass and microeukaryotic diversity. All analyses were carried out in triplicate.
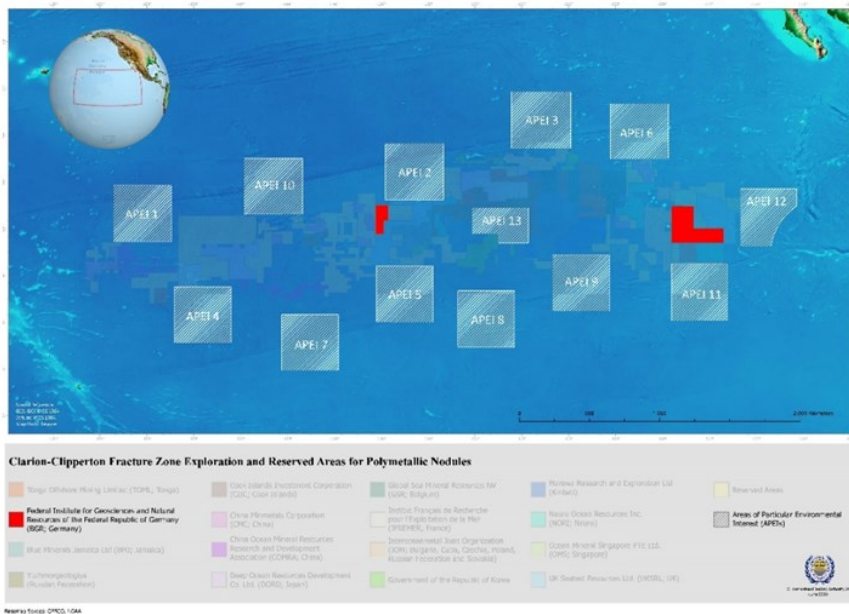
Figure 4: German contract areas for the exploration of manganese nodules within the Clarion–Clipperton Zone (CCZ). Investigated stations are located in the right red area near the APEIs 11 and 12 which are excluded from any mining activities (green shaded squares). Geographical data provided by the ISA.

Figure 5: Belgian contract areas for the exploration of manganese nodules within the Clarion–Clipperton Zone (CCZ). Investigated stations are located in the right white area near the APEIs 3 and 13 which are excluded from any mining activities (green shaded squares). Geographical data provided by the ISA.

2.2 Phytopigments concentration

The photosynthetic pigment concentration, used as a proxy of organic matter produced by photosynthesis in surface waters and supplied to the seafloor by sinking particles, was determined according to MacIntyre, Geider & Miller (1996); Montagna, Coull, Herring & Dudley (1983); Plante & Reys (1986).

An aliquot of sediment from each sample was collected in a glass tube with 0.1g of $MgCO_3$ and weighed, 10mL of 90% (vol/vol) acetone was added and the tubes once closed were shaken with a vortex and sonicated in the dark. Tubes were stored overnight at 4°C in the dark and then centrifuged (10 min at 800 x g). For the spectrophotometric assay (Chlorophyll-a estimation), 3 mL of the supernatant were pipetted into an optical glass cuvette and the absorbance was determined at 665 nm against a blank of 90% acetone. For phaeopigment measurement the acetone extract was acidified directly in the optical cuvette adding 200 μl of 0.1N HCl (Danovaro, 2010) and then the absorbance at 665 nm was read. The sum of chlorophyll-a and phaeopigment concentrations was expressed as total phytopigments concentration (CPE, *Chloroplastic Pigments Equivalent*) (Danovaro, 2010).

2.3 Organic matter composition

The concentration of proteins, carbohydrates, and lipids was measured spectrophotometrically (Danovaro, 2010), and the sum of the their concentrations converted into carbon equivalents (by using the conversion factors of 0.49, 0.40 and 0.75 mg C mg^{-1}, respectively) was defined as biopolymeric carbon (BPC) (Danovaro, 2010).

Biopolymeric C concentrations in the sediment were used as a proxy of availability of food for benthic consumers, whereas the protein to carbohydrate ratio was used as a proxy of its nutritional value (i.e. quality, Pusceddu et al., 2003, 2009).

2.3.1 Proteins concentrations

The protein extraction from sediment samples was conducted following the Hartree method (1972) adapted by Rice (1982). This method exploits the property of the protein to react with the cupric tartrate and subsequently with the Folin-Ciocalteu, which allows the obtainment of a blue colouration in the reaction solution that is proportional to the protein content. An aliquot of wet sediment from each sample was placed in a 15 mL glass tube with 1 mL of MilliQ water and shaken by using a vortex (1 min). The tubes were treated with ultrasound (Branson Sonifier 3510E; three for 1 min with 30s intervals). Then, 0.9 mL of solution A (2g of NaK-tartrate and 100g of Na_2Co_3

anhydrous in 500mL of 1 N NaOH, diluted to 1000mL with MilliQ water) were added to each tube and the tubes were incubated in a hot-bath (50°C) for 10 min. Subsequently, 0.1 mL of Solution B (2g of NaK-tartrate and 1g of $CuSO_4$ in 90 mL MilliQ water and diluted with 10 mL of 1N NaOH) were added, and the tubes were shaken with vortex (1min) and left at room temperature (10 min). Finally, 3 mL of Solution C (1 mL of Folin-Ciocalteau in 15 mL of MilliQ water) were added to each tube and the tubes were shaken with vortex (1 min) and placed in a hot-water bath (50°C) for 10 min. Tubes were centrifuged (15 min at 800 x g). About 3 ml of supernatant was collected and analysed spectrophotometrically at 650 nm. The protein content of the samples was obtained on the basis of a calibration curve prepared using the bovine albumin standard (BSA). Protein concentration was normalized to sediment dry weight and expressed as milligrams of BSA equivalent per gram of dry sediment.

2.3.2 Carbohydrate concentrations

The determination of carbohydrates was carried out according to the procedure of Dubois, Gilles, Hamilton, Rebers & Smith (1956) optimized for the sediment from Gerchakov & Hatcher (1972). This colorimetric method exploits the reaction between sugars and phenol in the presence of concentrated sulfuric acid. An aliquot of wet sediment from each sample was

placed in a 15 mL glass tube with 1mL of MilliQ water, shaken with vortex (1min) and sonicated three times (Branson Sonifier 3510E; 1min with 30s intervals). After sonication, 1 mL of a 5% distilled phenol solution was added to the tubes that were shaken with a vortex (1min) and incubated at room temperature (10 min). Then 5 mL of H_2SO_4 was added by using an automatic dispenser. This device was used because the reaction between the acid and the sediment carbonates may determine the development of CO_2 bubbles. Tubes were closed and centrifuged (30 min at 800 x g). About 3 ml of supernatant were collected and analysed spectrophotometrically at 485 and 600 nm. Carbohydrate concentrations were obtained by calibration curves of standard solutions of D (+) glucoseand expressed as mg per g of sediment dry weight.

2.3.3 Lipid concentrations

The determination of total lipid concentration in sediment samples was carried out according to Bligh & Dyer (1959) and J.B. Marsh & Weinstein (1966), slightly modified to be applied to the sediment matrix (Danovaro et al., 2010). An aliquot of wet sample was placed in a glass tube adding 1 mL of MilliQ water. Tubes were shaken with vortex (1min), sonicated three times (Branson Sonifier 3510E; 1min with 30s intervals) and centrifuged (800x g for 10 min). The hydroalcoholic fraction of the supernatant was removed by using a Pasteur pipette and placed into Pyrex glass tubes adding 1.25mL of

chloroform and 1.25mL of MilliQ water. The tubes were vortexed to produce water-methanol-chloroform emulsion and centrifuged at 800 x g for 5 min in order to separate the hydrophobic and the hydroalcoholic fractions. This latest one was eliminated and the hydrophobic residual was allowed to evaporate in a dry hot bath (for 20 min at 100°C). Once 2 mL of H_2SO_4 was added at room temperature, the tubes were placed in a dry hot bath for 15 min. After the reaction the acid turned to a light yellow or brown colour. The tubes were transferred into a wet bath (at room temperature, for 15s) and then into an ice bath (at 0°C for 5 min). Then, 3 mL of MilliQ water were added and the tubes were shaken with vortex (1 min). The supernatant was analysed spectrophotometrically and the absorbance was determined at 375 nm. Each absorbance value was compared to the absorbance of MilliQ water used as blank. The sediment dry weight was calculated as the difference between the initial weight of the empty glass tubes and the tubes after sediment desiccation (24h at 60°C). The total lipid concentration was calculated on the basis of calibration curves obtained by analysing standard solutions of tripalmitin. Total lipid concentration was normalized to sediment dry weight.

2.4 Prokaryotic abundance and biomass

Total prokaryotic counts were performed using the SYBR Green I direct count procedure (Danovaro, 2010). Briefly, the sediment samples were treated by ultrasounds (Branson Sonifier 2200, 60W) three times for 1 minute after addition of 0.2 µm pre-filtered tetrasodium pyrophosphate solution (final concentration, 5 mM), then properly diluted before filtration onto 0.2 µm pore-size Nuclepore black filters (Whatman). Filters were then stained with 20 µl of SYBR Green I (10000× stock) diluted 1:20 in pre-filtered TE buffer (pH 7.5), with excess stain removed 3 times using 3 ml of Milli-Q water, and mounted onto microscope slides. At least 20 microscope fields and 400 cells per filter were counted randomly using epifluorescence microscopy under blue light. For the determination of the prokaryotic biomass, prokaryotic size was converted into bio-volume following inter-calibration with Scanning Electron Microscope (SEM) based size determinations and converted into carbon content assuming 310 fgC µm-3 (Danovaro, 2010), in line with previous studies (Rastelli et al., 2016 and ref. therein).

2.5 Extracellular enzymatic activities

The degradation potential of organic matter by prokaryotes was assessed through the analysis of the main extracellular enzymatic activities (EEA).

Extracellular enzymatic activities determined for aminopeptidase and β-glucosidase were determined by the analysis of the cleavage rates of the fluorogenic substrates L-leucine-4- methylcoumarinyl-7-amide (Leu-MCA) and 4-methylumbelliferyl (MUF)-b-D-glucopyranoside (Glu-MUF), respectively (Sigma Chemicals) under saturating substrate concentrations (Danovaro, 2010). Briefly, sediment sub-samples were diluted with 0.2-μm pre-filtered seawater and each mesocosm were incubated in the dark at the *in-situ* temperature for 1 hour. The fluorescence of the samples was measured fluorometrically (380:440 nm and 365:455 nm, excitation:emission, for Leu-MCA and Glu-MUF, respectively) immediately after the addition of the substrate and after the incubation, and converted into enzymatic activity using standard curves of 7-amino-4-methylcoumarin for Leu-MCA and 4-methylumbelliferone for Glu-MUF (Sigma Chemicals).

The amount of the artificial fluorogenic substrate enzymatically hydrolyzed by proteases and glucosidases, was converted into protein or carbohydrate degradation rates using 72 μg of C per micromole of substrate hydrolyzed. The turnover times of proteins and carbohydrates, used as a proxy of organic matter cycling, were calculated as the ratio of the protein and carbohydrate carbon concentrations and their degradation rates converted into carbon equivalents (Danovaro, 2010).

2.6 Viral abundance and production

According to Danovaro (2010), the sediment samples were sonicated three times (Branson Sonifier 2200, 60W) for 1 minute after addition of 0.02 μm pre-filtered tetrasodium pyrophosphate solution in seawater (final, 5 mM). In order to eliminate uncertainties in virus counting due to extracellular DNA interference, sub-samples were supplemented with DNase I from bovine pancreas (5 U mL^{-1} final concentration) and incubated for 15 min at room temperature. The samples were properly diluted with 0.02-μm pre-filtered seawater, filtered onto 0.02-μm-pore-size Al2O3 filters (Anodisc; diameter 25 14 mm) and then stained with 100 μl of SYBR Gold 2x (diluting stock solution with 0.02-μm pre-filtered TE buffer: 10 mM Tris-HCl, 1 mM EDTA). Filters were incubated in the dark for 20 minutes, rinsed three times with 3 ml of 0.02-μm pre-filtered Milli-Q water, dried under laminar flow hood and then mounted on glass slides with 20 μl of antifade solution (50% phosphate buffer pH 7.8, 50% glycerol, 0.5% ascorbic acid). Viral counts were obtained by EFM under blue light (Zeiss Axioskop 2MOT, magnification × 1,000) examining at least 20 fields per slide, and at least 400 viral particles per filter. Viral production was determined by time-course experiments of sediment samples previously diluted with virus-free seawater (0.02 μm pre-filtered), collected at the sediment-water interface of each

benthic site (Rastelli et al., 2016). Replicate samples (n=3) for viral counts were collected immediately after dilution of the sediments and after up to 12 h incubation in the dark at *in-situ* temperature. Subsamples were then analyzed as reported above for the determination of viral abundance. The viral production rates were determined from linear regression analyses of the increase of viral abundances over time (Dell'Anno et al., 2009), and data were normalized to sediment dry weight after desiccation (48 h at 60°C).

2.7 Microeukaryotic DNA extraction and purification

Before the extraction of total DNA, 2 g of wet sediments samples was pre-treated with three previous washing solutions according to Danovaro et al. (2010) to increase DNA yield and purity. Sediment samples were resuspended with 5 ml of Wash solution 1 (50mM Tris-HCl; pH 8.3; 200 Mm NaCl; 5 Mm Na2EDTA; 0.05% Triton X-100), vortexed and centrifuged at 6000x g for 2 minutes. Ones discarded the supernatants, the pellets were washed with a: Wash solution 2 (50mM Tris-HCl; pH 8.3; 200 Mm NaCl; 5 Mm Na2EDTA), treated as described above between each washing, and resuspended with a Wash solution 3 (10 mM Tris-HCl; pH 8.3; 0.1 mM Na2EDTA).

UltraPure water was used: reagent-grade water, previously autoclaved, filtered (through 0.2μm, better 0.02μm) and stored in sterile 2ml Eppendorf tubes at 4°C.

After the washing procedure, total DNA was extracted from ~0.5 g of the resulting pellets using the Powersoil DNA isolation kit (QIAGEN) following manufacturer instructions.

Cell lysis occurs by mechanical force (beads tubes provided by the kit) and chemical reactions (kit solution C1). Total genomic DNA is captured at the end of the protocol on a silica membrane in a spin column format and eluted after the addition of an elution buffer (solution C6).

Total DNA quantification was done using the Spectrofluorimeter NanoDrop *1000*.

After the quantification, preliminary analyses to evaluate amplification efficiency of the 18S RNA gene through a PCR reaction. The primer set TAReuk454FWD1 (CCAGCASCYGCGGTAATTCC) and TAReukREV3mod (ACTTTCGTTCTTGATYRATGA) was used to amplify the V3 region of 18S RNA gene (Stoeck et al., 2010).

The reaction was carried out on the Veriti™ 96-Well Thermal Cycler in a 50 μL final volume with 10 μL MyTaq Reaction Buffer 5x, 0.25 μL of primers 515F-Y and 926R (0.5μM final concentration), 1 μL myTaq HS DNA

Polymerase (Meridian Bioscience), 1μL of template DNA and nuclease-free water pre-filtrated through a 0.02 μm pore size filter. The PCR program consisted of an initial denaturation step (95°C for 5 min), 10 cycles of annealing step (94°C for 30 sec, 57°C for 45 sec, 72°C for 1 min), 29 cycles of elongation step (94°C for 30 sec, 47°C for 45 sec, 72°C for 1 min), at the end the Polymerase was denatured at 72°C for 10 min.

After the amplification, for visualizing the DNA fragments, an electrophoretic run was done using agarose gel (1.5 %). The Invitrogen™ 100 bp DNA Ladder (ThermoFisher Scientific) with 13 fragments ranging from 100 to 200bp was utilized as marker.

2.7.1 Microeukaryotic DNA sequencing

For the analysis of microeukaryotic diversity, the V3 region of 18S RNA gene was amplified using the primer set TAReuk454FWD1 (CCAGCASCYGCGGTAATTCC) and TAReukREV3mod (ACTTTCGTTCTTGATYRATGA) (Stoeck et al., 2010) and the amplicons sequenced on Illumina MiSeq platform by LGC group (Berlin, Germany). Paired-end sequences were subsequently analyzed through the DADA2 procedure QIIME2) (Bolyen et al., 2019) to infer biologically significant Amplicon Sequence Variants (ASVs). The resulting ASVs were then

compared against the SILVA 18S database (v138.1; Quast et al., 2013; Yilmaz et al., 2014) for taxonomic affiliation using the VSEARCH-based inference plugin within QIIME2 (Bolyen et al., 2019) after trimming the reference sequences to the region amplified by the primers.

Prior to table rarefaction, metazoan-affiliated sequences were filtered from the resulting ASV table with the microeco package (Chi et al., 2021; RStudio software v 4.2.0).

The resulting ASVs table was filtered using the phyloseq package (McMurdie and Holmes, 2013; RStudio software v 4.2.0) to taxa seen at least two times in at least 5% of samples.

Alpha-diversity indices (i.e., ASVs Observed, Shannon index and Pielou Index) were calculated through the microbiome package (Lahti et al., 2017) within RStudio software (v 4.2.0). The main beta-diversity calculations were performed in vegan (Clarke et al., 1993, Warton et al., 2012) within R studio (software 4.2.0).

Taxonomic inference of ASVs was carried out using phyloseq package (Mcmurdie and Holmes 2013) considering taxa contributing at least 0.5% to the whole assemblage merging the remaining taxa into a single "Others" group. Microeukaryotic sequences were assigned to phylum and family level (unknown families were grouped at the lowest taxonomic level known).

2.8 Statistical analyses

Statistical analyses were prior transformed in square-root pre-treatment and then carried out on Bray-Curtis Distance similarity matrices using the PERMANOVA routine included in the Primer 6+ software package (Anderson, 2005). Post-hoc pair-wise comparisons were carried out when significant ($p < 0.05$) differences were encountered.

3. Results

3.1 Biochemical composition of sedimentary organic matter

Vertical patterns of chlorophyll and phaeopigments concentrations before the impact displayed a significant decrease with depth in the two investigated areas (PERMANOVA, $p<0.05$: Figure 6). After the mining impact, a significant decrease in chlorophyll was observed in the Belgian area (PERMANOVA, $p<0.005$; Figure 6B) and a significant decrease in phaeopigments was observed in both the German and Belgian Areas (PERMANOVA, $p<0.001$; Figure 6C and Figure 6D) with the strongest decrease in the first layer for the German Area (on average 2.28 ± 0.23 and 1.07 ± 0.08 µg/g respectively before and after the impact) and in all the layers for the Belgian Area.
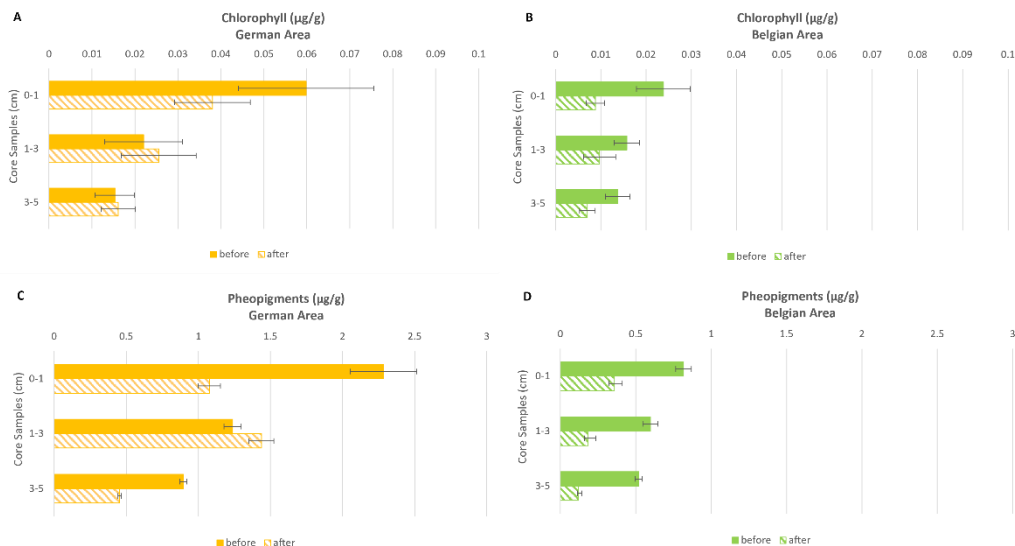

Figure 6: *Mean values and standard error of chlorophyll and phaeopigments concentrations along the vertical profile of sediments collected in sites of the German (yellow) and Belgian (green) area before and after the impact.*

Integrated values of CPE (*Chloroplastic pigments equivalent*) concentrations
down to 5 cm of sediment, are reported in Figure 7.

Before the mining impact, German and Belgian areas displayed differences in
phytopigment concentrations (PERMANOVA, *p<0.001*). After the impact, a
significant decrease in CPE (PERMANOVA, *p<0.001*) was observed in both
the German and Belgian areas with the strongest decrease in the Belgian area
(CPE on average 0.66±0.04 and 0.22±0.02 µg/g respectively before and after
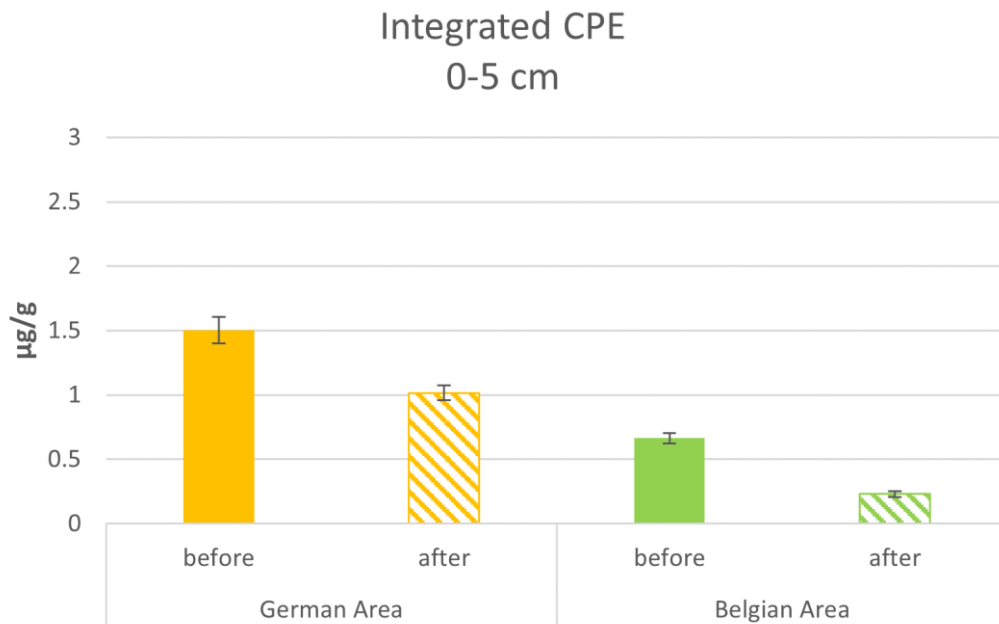the impact).

*Figure 7: CPE integrated concentrations and standard error in German (yellow) and
Belgian (green) areas before and after the impact.*

Vertical pattern of protein concentrations before and after the impact displayed a significant decrease with depth in the German area (*PERMANOVA*, p<0.05; Figure 8A). Both German and Belgian areas displayed significant differences in protein concentrations before and after the mining impact (*PERMANOVA*, p<0.001; Figure 8A and Figure 8B).

Carbohydrate represents the major fraction of the total biopolymeric carbon (BPC) in both the investigated areas (Figure 8C and Figure 8D). Vertical pattern of carbohydrates concentrations before and after the impact displayed a significant decrease with depth in the two investigated areas (*PERMANOVA*, p<0.05; Figure 8C and Figure 8D). After the mining impact, a significant decrease in carbohydrates was observed in Belgian area (*PERMANOVA*, p<0.001; Figure 8D).

Lipid concentrations along the sediment's vertical profile and also before and after the mining impact both in German and Belgian areas (Figure 8E and Figure 8F) revealed the lack of significant differences between sites (*PERMANOVA*, p>0.05).
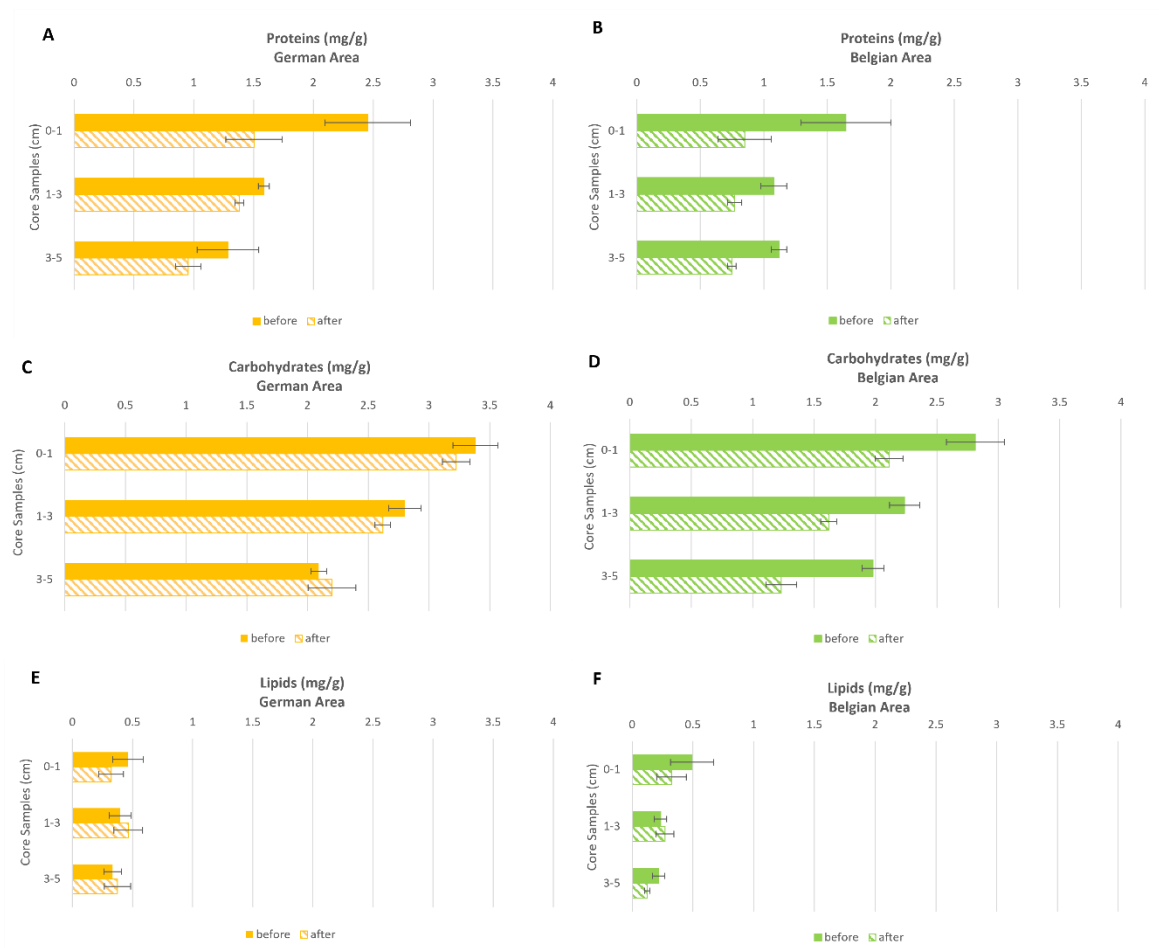
Figure 8: Mean values and standard error of biochemical concentrations along the vertical profile of the sediments collected in German (yellow) and Belgian (green) sites before and after the impact. In the figure are shown proteins (A and B), carbohydrates (C and D), lipids (E and F).

Integrated values of BPC (*Biopolymeric Carbon*) concentration down to 5 cm of sediment, and BPC concentration in the upper horizon are reported in Figure 9.

Before the mining impact, German and Belgian areas displayed differences in Biopolymeric carbon (*PERMANOVA*, $p < 0.001$). After the impact, a significant decrease in BPC (*PERMANOVA*, $p < 0.01$) was observed in both the German and Belgian areas considering both the first horizon and the integrated ones with the strongest decrease in the Belgian area (0-5 cm BPC on average 1.84 ± 0.17 and 1.22 ± 0.06 mg/g respectively before and after the impact).
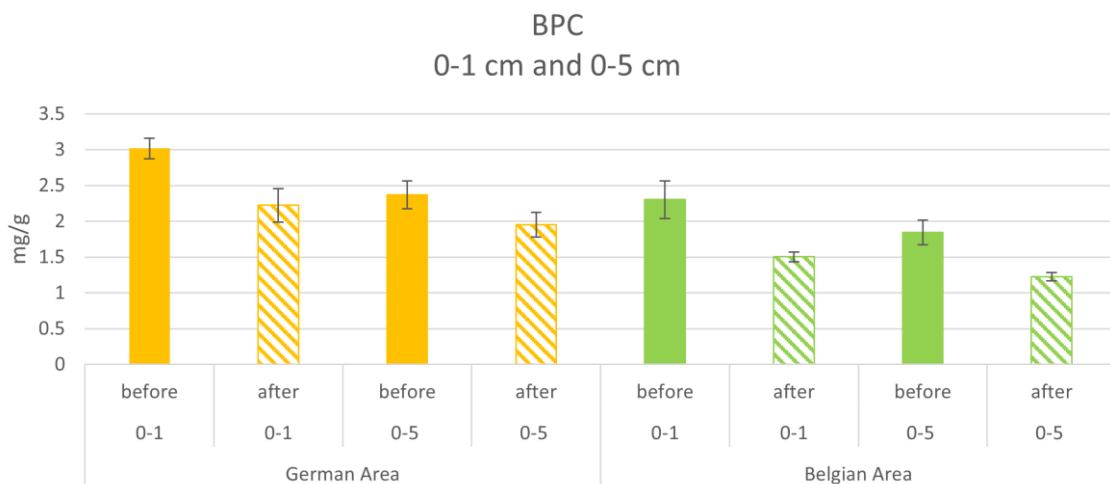

Figure 9*: BPC concentration in the first horizon, integrated concentrations and standard error in German (yellow) and Belgian (green) areas before and after the impact.*

3.2 Prokaryotic abundance and biomass

Comparing prokaryotic abundance of the top 1st cm of sediments, (Figure 10A) in the two areas before the seafloor disturbance experiment cell number was significantly higher in the German than in the Belgian Areas before the mining impact (PERMANOVA, *p<0.001*). Prokaryotic cells in the German Area were two times lower after the impact (on average $2.64x10^7 \pm 3.10x10^6$ and $1.34x10^7 \pm 1.07x10^6$ cells g^{-1} respectively before and after the impact), while in the Belgian Area higher values were observed after the impact $(3.82x10^6 \pm 2.67x10^5$ and $9.39x10^6 \pm 1.48x10^6$ cells g^{-1} respectively before and after the impact). A similar pattern was observed, in the first centimetres, for prokaryotic biomass (Figure 10B) with higher biomass in the German than in the Belgian Areas (PERMANOVA, *p<0.001*; on average $3.95x10^{-1} \pm 6.07x10^{-2}$ and $5.39x10^{-2} \pm 6.26x10^{-3}$ µgC g^{-1} respectively for German and Belgian before the impact).
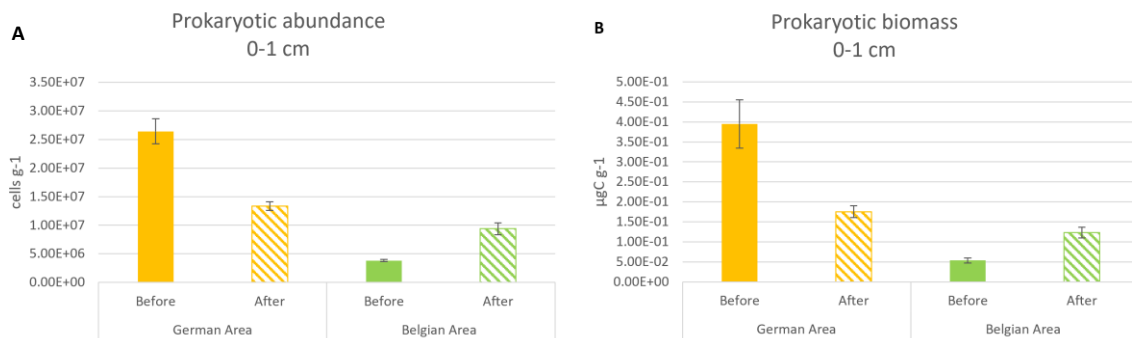

Figure 10: *Mean values and standard error of prokaryotic abundance (A) and biomass (B) in surface sediments of before and after impact sites of each study area, are reported. Data are expressed as number of cells per gram (dry weight) of sediment for prokaryotic abundance and in µgC per gram (dry weight) of sediment for prokaryotic biomass.*

3.3 Extracellular enzymatic activities and protein turnover time

Vertical patterns of Aminopeptidase and β-Glucosidase activities before the impact displayed significant differences along the vertical profile in the two investigated areas (PERMANOVA, *p<0.05*; Figure 11).

Aminopeptidase activity (Figure 11A and 11B) were always higher than β-glucosidase activities in both the investigated areas and significantly decrease with the depth of the sediments (PERMANOVA, *p<0.05*).

β-Glucosidase activity (Figure 11C and 11D) showed different patterns between the two investigated areas. In the German area it displays a significant decrease along the vertical profile (PERMANOVA *p<0.05*; Figure 11C); in the Belgian area an opposite pattern is showed with a significant increase along the vertical profile before the mining impact (PERMANOVA, *p<0.05*; Figure 11D) and a significant reduction in the deepest core's horizon after it (PERMANOVA, p<0.05).
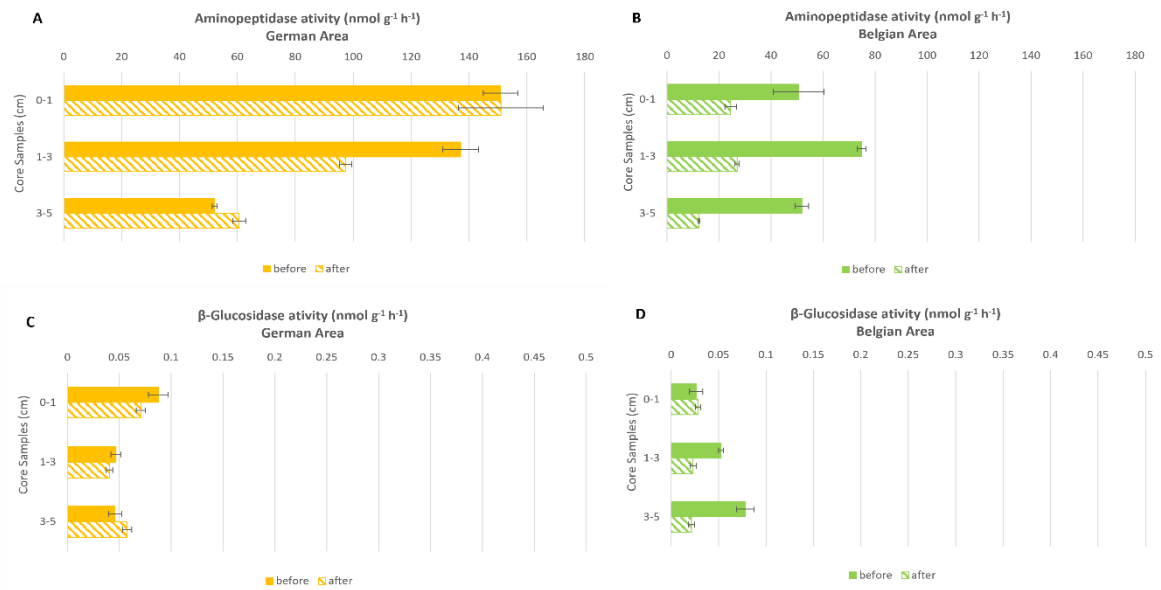
Figure 11: *Aminopeptidase (A and B) and β-glucosidase (C and D) activity and standard error along the vertical profile of the sediments collected in German (yellow) and Belgian (green) sites before and after the impact.*

Integrated values of Aminopeptidase (MCA) and β-Glucosidase (β-Glu) activities down to 5 cm of sediment both in German and Belgian areas, are reported in figure 12A and 12B, respectively.
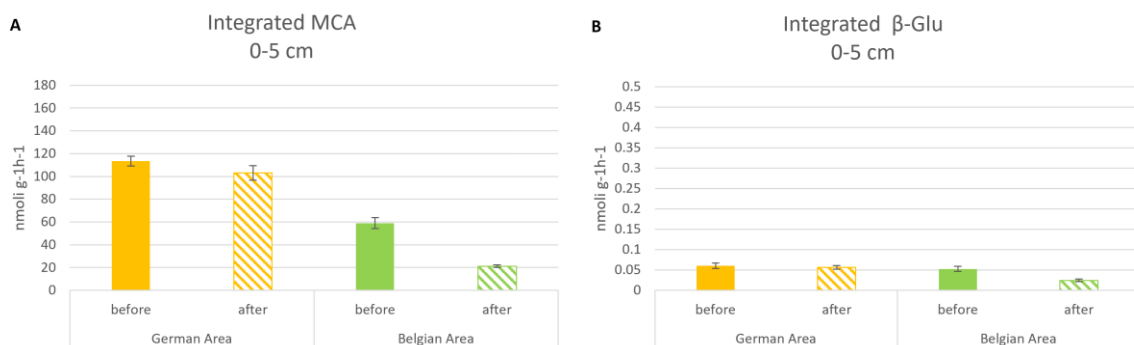

Figure 12: *Mean values of Integrated Aminopeptidase (E) and β-Glucosidase activity and standard error in German (yellow) and Belgian (green) areas considering both the before and after impact.*

Before the mining impact, German and Belgian areas displayed differences in Aminopeptidase and β-Glucosidase activities (PERMANOVA, *p< 0.001*; Figure 12). After the impact, a significant decrease both in Aminopeptidase (PERMANOVA, *p<0.001*; Figure 12A) and β-Glucosidase (PERMANOVA, *p<0.001*; Figure 12B) was observed in the Belgian area (Aminopeptidase on average 59±4.69 and 21.19±1.12 nmoli g^{-1} h^{-1} respectively before and after the impact; β-Glu on average 0.05±0.006 and 0.02±0.003 nmoli g^{-1} h^{-1} respectively before and after the impact), in the German area a significant decrease was not observed.

Total protein turnover time of the top 1st cm and down to 5 cm of sediment both in German and Belgian are reported respectively in figure 13A and 13B. Before the mining impact, German and Belgian areas displayed differences in the degradation rate of protein content (PERMANOVA, *p< 0.05*; Figure 13) with a longer turnover-time in the Belgian area. After the impact, a significant decrease was observed in the German area with the strongest decrease in the top 1 cm horizon (Turnover-time on average 6.51±1.01 and 3.14±0.20 days respectively before and after the impact; Figure 13A); in the Belgian area an opposite pattern was displayed with a significant increase of days in the

degradation rate of protein content (PEMANOVA, *p<0.05*) after the impact in the integrated core's horizon (Figure 13B).
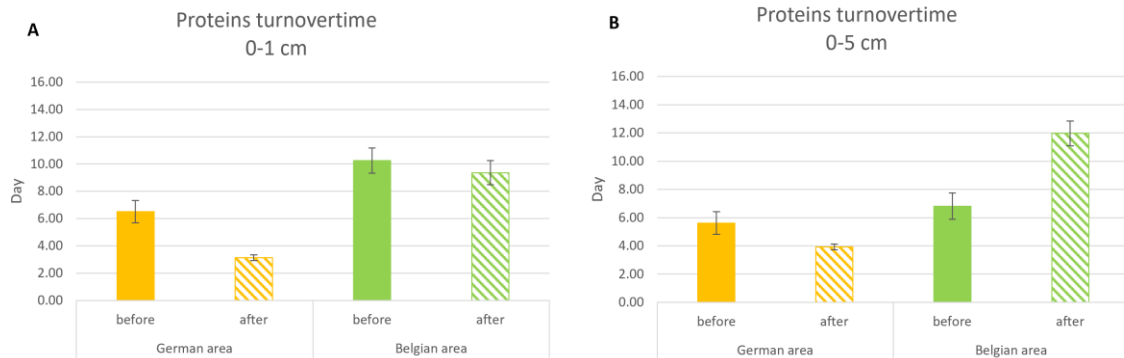

Figure 13: *Mean values and standard error of protein turnover time in surface sediments and down to 5 cm of before and after impact sites of the study areas.*

3.4 *Viral abundance and production*

Comparing the viral abundance of the top 1st cm of sediments, (Figure 14A) in the two areas before the seafloor disturbance experiment cell number was significantly higher in the German than in the Belgian Areas before the mining impact (PERMANOVA, $p<0.05$).

Viral abundance (Figure 14A) showed the highest number of viruses in the German area in which the abundance decreases significantly after the impact (PERMANOVA, $p<0.001$; Figure 14A); in the Belgian area, a significant decrease of the abundance is not observed.

Viral production (Figure 14B) in the top 1st cm of sediment, showed an opposite pattern between the two areas with the highest viral production in the Belgian area.

In both German and Belgian areas the viral production decreased after the impact; in the Belgian area viral production are significantly different before and after the impact (PERMANOVA, *p<0.001*; Figure 14B).
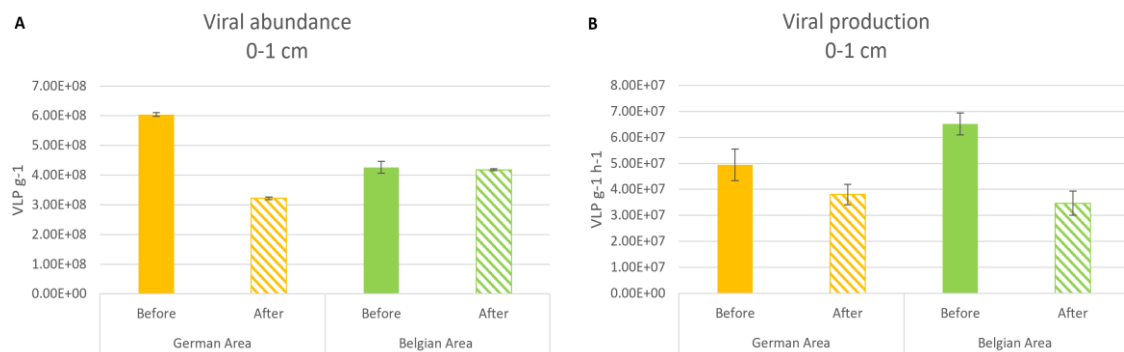

Figure 14: *Mean values and standard error of viral abundance (A) and production (B) in surface sediments of before and after impact sites of each study area, are reported. Data are expressed as number of viruses per gram (dry weight) of sediments for viral abundance and as number of viruses per gram (dry weight) of sediments produced per hour for viral production.*

3.5 Microeukaryotic diversity and taxonomic identification

The observed ASVs (Figure 15A) showed significant differences between the two investigated areas before the mining impact (PERMANOVA, *p<0.05*). Both German and Belgian areas displayed high spatial variability with unclear pattern between before- and after-impact.
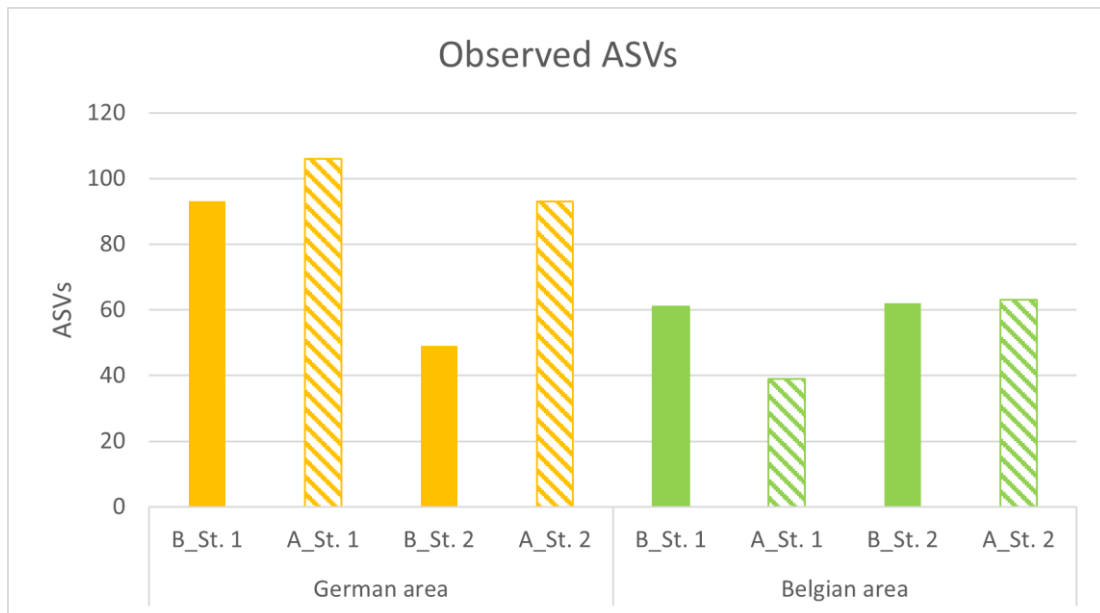
Figure 15: *alpha diversity considering observed ASVs.*

The grouping of the analysed samples based on the taxonomic classification of the benthic microeukaryotic assemblages, is illustrated in Figure 16 and 17. PCoA analyses (Principal Component Analyses, Figure 16) showed that microeukaryotic assemblages found in the German Area and Belgian areas clustered separately before and after the disturbance experiment (PERMANOVA, *p<0.01*).

In the Belgian area the taxonomic composition clustered separately before and after the impact (*PERMANOVA, p<0.05*), while in the German Area microeukaryotic assemblages did not display significant differences.

Figure 16: Principal component analyses (PCoA) shows the inter-sample distances between the German and Belgian Areas before and after the mining impact.

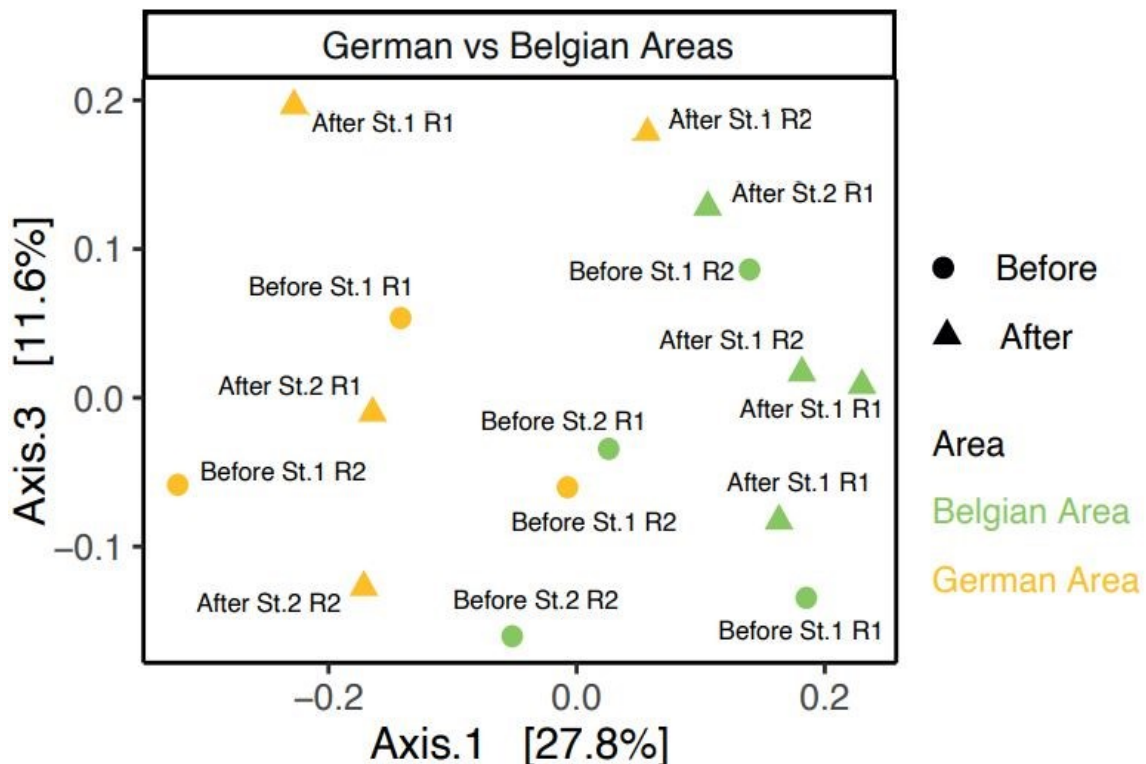*Ascomycota* is the most abundant phylum in the benthic microeukaryotic assemblage both for the German and Belgian areas contributing on average to 61.1% before and 68.5% after the impact in the German area and on average to 67.6% before and 49.4% after the impact in the Belgian Area.

Protalveolata phylum is the second most abundant phylum in the German Area and accounted on average for 19.7% before the impact and 14.9% after the impact. In the Belgian area, before the impact *Cercozoa* is the second most abundant phylum (10.7%), while after the impact the second most abundant phylum was the *Protalveolata* (18.1%).

In both German and Belgian Area*, Metschnikowiaceae* was the dominant family in all the sediment samples accounting on average for 61% before the impact and 68.2% after the impact in the German area and on average for 66.8% before the impact and 49.4% after the impact in the Belgian area (Figure 17).

The ASVs contributing at least 0.5% to the whole assemblages were merged in the "Others" group (figure 17).
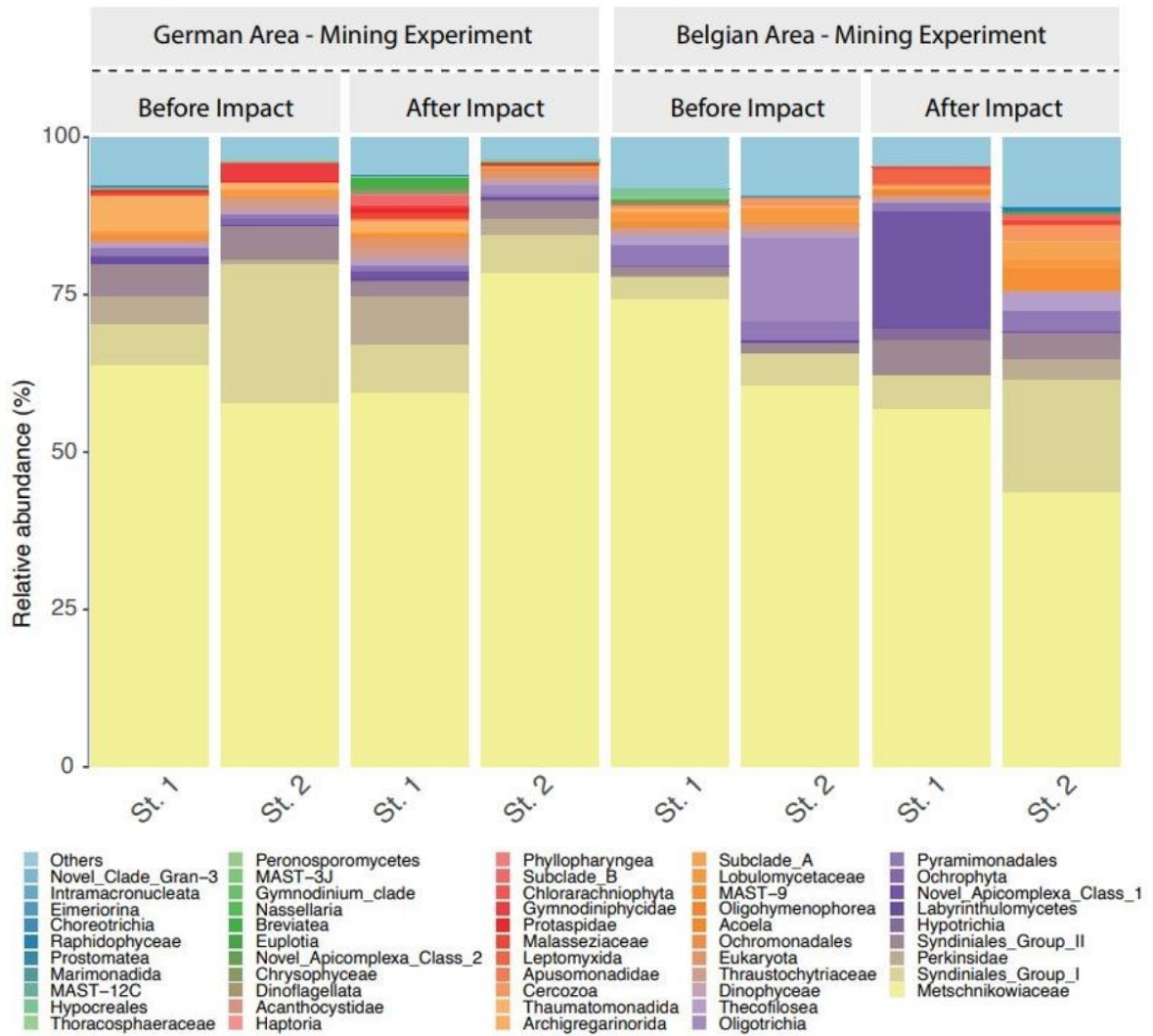
Figure 17: *taxa Bar-Plot shows the relative abundances of taxa present in the two areas before and after the impact.*

4. Discussion

With the global raw materials crisis, the need to identify alternative sources of certain essential minerals is becoming increasingly evident, and among these, the presence of polymetallic nodules on abyssal seafloor is undoubtedly one of the most interesting resource exploitations from an industrial point of view. At present, however, it seems clear that the extraction of polymetallic nodules risks being extremely impactful to such an extent that it does not comply with the DNSH 'Do No Significant Harm' principle that underlies sustainable development (PNRR-salute.gov.it).

The two investigated areas (German and Belgian) showed significant differences in organic matter content and composition, extracellular enzymatic activities, and microbial assemblages (in terms of prokaryotic abundance and biomass, viral abundance and production and microeukaryotic diversity).

The significant differences observed in terms of organic matter content and composition highlight the different trophic characteristics in the two investigated areas. Previous evidence reported that the CCZ is subjected to spatial differences in C fluxes to the seafloor with the German area subjected to a greater C supply than the Belgian area (Lutz et al., 2007).

Trophic differences between these two different areas, are confirmed by the evidence of different amounts of phytodetritus (here quantified through the proxy of phytopigments and chlorophyll-a) deposited on the seafloor.

The analysis of the results clearly indicates that deep-sea mining (here simulated by means of the Patania II hydraulic prototype) had significant effects on benthic ecosystems.

Comparing values of the sediment variables before and after the simulated impact of mining activities, we observed consistent results in both the German and Belgian investigated areas. The most evident effect was the decrease of concentration of phytopigments and other biochemical components of the sediment organic matter. For instance, the protein concentration decreases significantly down to 5 cm depth. The decrease in protein content was more evident, up to ca 50% in the first centimetre of the Belgian area, but the effects were evident down to at least 5 cm depth, the deepest sediment horizon at which the the analyses were carried out.

The before-after comparison for carbohydrate concentrations revealed the similar patterns in both in the German and Belgian areas.

In the Belgian area these changes appear more evident in terms of average concentrations down to a depth of 5 cm core's horizon, whereas they appear no more significant at the same depth in the sediment from the German area.

Lipids are a component that show a lower concentration, however, at least for the shallowest 0-1 cm layer, the results indicate a consistent trend with that of the other biochemical components of organic matter, with a strong decrease in the average concentration of lipids.

These data indicate that the mechanical effect of mining activities conducted by Patania II leads to a 'food depletion', i.e. a decrease in the availability of organic matter for consumers.

Such effects would therefore result in more hostile conditions of deep environments for the abyssal fauna, already stressed by the low concentrations of organic matter available to deposit-feeding assemblages and other organisms that utilise these food sources.

These data are evident not only in the first centimetre of the core horizon, but also by integrating the first 5 cm, which indicates how much the organic matter as a whole (BPC) has been depleted by more than 20-30% suggesting a profound change in the most bioactive benthic compartment.

The effect of the decrease in trophic availability brought by Patania II, is certainly due to a mechanical sediment reworking determining the sediment resuspension and the export of the surficial OM deposits.

This is evident from the fact that, even though the survey site is around 4500 metres deep, and thus is not characterised by the presence of *in-situ*

photosynthetic primary production (Danovaro et al., 2008), it nevertheless receives a "rain" senescent and dead phytoplankton (i.e., chlorophyll-a and total phaeopigments) and other organic detritus (Glover and Smith, 2003). The concentrations of chlorophyll-a, in particular, appears extremely low and almost undetectable, but it is evident that these are in any case resuspended by mining activities and probably swept away.

This is also evident for the overall concentration of phaeopigments in both the German and Belgian areas, where the effect of the Patania II passage on the surface layer is such that these concentrations decreased by ca 50%.

These data tell us that the passage of Patania II and mining activities cause the re-suspension of organic matter, both in terms of labile biochemical components and biomass of fresh detritus (photosynthetic pigments).

These aspects were compared with the effects on microbial components which processes provide essential benefits, driving the nutrient regeneration and global biogeochemical cycles that are fundamental to sustain not only the key-processes in the deep-sea ecosystem but also to sustain primary and secondary production (Gage and Tyler, 1991); the effects on prokaryotic abundance and biomass were analysed.

The German area, characterised by higher amount of organic matter than the Belgian area, reaches abundances in the order of about $0.2\text{-}0.3 \times 10^8 \pm 0.02 \times 10^8$

cells per gram of sediment, while it reached values 5 times lower in the Belgian area. A halving in prokaryotes abundance and biomass is observed in the German area, which seems to undergo an effect that similar to that observed for photosynthetic pigments and other components of organic matter. This decrease in prokaryotic abundance is also reflected in their biomass and in a decrease in viral abundance which in the German area halves after the passage of Patania II, while it decreases only modestly in the Belgian area.

The parallel decrease in viral production, between before and after mining activity, indicates that mining activities had an overall negative impact on microbial activities and production, since viral production activity typically results with the combined effect of prokaryotic abundance (particularly host cell activity).

These data are supported by the analysis of enzymes, aminopeptidase and β-glucosidase activities. Protease activity in particular is a measure that typically correlates very closely with prokaryotic activity, so that a consistent pattern is anticipated.

Enzymatic activities, decreased after the passage of Patania II, with a more marked decrease in the Belgian area.

Overall, a decrease in microbial activity and abundance, which is associated with a decrease in viral activity (and thus in the killing and turnover capacity of microbial cells) and a decrease in enzyme activity, suggest that the mechanical effect of Patania II is such that it can also alter biogeochemical cycles.

This effect is highly interesting because, in past studies, trawling activities (which are also activities that lead to an alteration of the integrity of the surface layer of the sediment, the re-suspension of sediment plumes and the alteration of the composition of biogeochemical cycles) reported an increase in protein concentration due to mobilisation effects and a stimulation of microbial activity precisely due to the sedimentary stirring brought about by sediments mobilisation effects (Pusceddu et al., 2014); although the consequences of trawling can be variable dependently on the ecosystem considered (Fiordelmondo et al., 2003). Therefore, the originality of these results lies above all in this effect: an effect that not only determines a 'food depletion' of the food supply but also a variation of the biogeochemical processes of mineralisation of organic matter.

A further area of investigation at this point turned to the micro-eukaryotic component, which was carried out using bar-coding sequencing techniques that reveal a simultaneous variation (in both the German and Belgian

samples) in the diversity of the micro-eukaryotic component between before and after the seafloor disturbance experiment.

As approximately 20 to 40 hours elapsed between pre-impact and post-impact sampling, the data seem to indicate that, at least on a short time scale, a generally negative effect found on the prokaryotic component also manifests itself on the microeukaryotic component. The most likely hypothesis related to the mechanical impact of the Patania II passage is that of disturbance which caused shifts in microeukaryotic taxa probably related to sediment resuspension and/or an increase in mortality of some taxa. Analysis of the taxa bar-plot shows variations in the percentage composition of the dominant groups in the before-impact and after-impact conditions (i. e. phylum *Ascomycota* and family *Metschnikowiaceae* on average of ~ 65% before and ~ 60% after the impact). Although there is clear variability between different samples and significant distance in the cluster division between the two areas, in both cases there is a clear shift in composition; thus not only in the number of taxa but also in the composition of the taxa themselves (i.e. families of *Metschnikowiaceae* and *Syndiniales* became more abundant after the impact in the two investigated areas). It is also possible that certain shifts in the composition of the microeukaryotic community are due precisely to those components that opportunistically manage to utilise material released by the

mortality of certain organisms; which is not such as to determine a positive effect on the availability of organic material, but which does, however, determine the availability of material that can potentially be utilised by these opportunistic components.

5. Conclusions

The results of this study highlight that mining activities can cause significant alterations not only in the trophic state of the deep-sea benthic system, but also in terms of microbial assemblages and in the virus-host interactions.

A significant alteration is evident also in the availability of organic matter for consumers, in particular deposit-feeders, probably associated with the effects of re-suspension and the creation of sediment plumes. A decrease in prokaryotic abundance and activity as well as in enzymatic activities and consequently in the biogeochemical cycles of organic matter can also be observed (for the first time in connection with mechanical disturbance events).

These processes are also reflected in an alteration in the diversity of microeukaryotic components that is consistent in the two areas, and in an increased dominance of certain groups.

The results of this experiment are evident because they represent the results of a unique experimental activity conducted at a depth of 4500 metres using the first semi-industrial collector prototype never tested before.

Even though the two areas, distant to each other 1000 km, are characterized by quite evidence differences in trophic resources before the impact, the effect of mining activities on them is the same. However, the two areas, respond differently in their microbial component.

In conclusion, these results confirm the fact that extreme caution should be exercised in performing deep-sea mining activities because the impacts of mineral extractions would involve all the benthic compartments in different ways according to different areas, but could also affect biogeochemical processes that are at the basis of the sustainability and functioning of the oceans.

6. REFERENCES
Sites

1. Home - JPIO Mining Impact (geomar.de)

2. DeepCCZ: Deep-sea Mining Interests in the Clarion-Clipperton Zone: NOAA Office of Ocean Exploration and Research

3. Home | International Seabed Authority (isa.org.jm)

4. Maps | International Seabed Authority (isa.org.jm)

5. BGR - MiningImpact logbook 2021 (bund.de)

6. Principio DNSH (salute.gov.it)

Bibliography

1. Beaudoin, Y. and Baker, E., 2013. Deep Sea Minerals: Manganese Nodules, a Physical, Biological, Environmental and Technical Review.

2. Bligh, E.G. and Dyer, W.J., 1959. A rapid method of total lipid extraction and purification. *Canadian journal of biochemistry and physiology*, *37*(8), pp.911-917.

3. Bluhm, H., 2001. Re-establishment of an abyssal megabenthic community after experimental physical disturbance of the seafloor. *Deep Sea Research Part II: Topical Studies in Oceanography*, *48*(17-18), pp.3841-3868.

4. Bolyen, E., Rideout, J.R., Dillon, M.R., Bokulich, N.A., Abnet, C.C., Al-Ghalith, G.A., Alexander, H., Alm, E.J., Arumugam, M., Asnicar, F. and Bai, Y., 2019. Reproducible, interactive, scalable and extensible microbiome data science using QIIME 2. *Nature biotechnology*, *37*(8), pp.852-857.

5. Canals, M., Puig, P., de Madron, X.D., Heussner, S., Palanques, A. and Fabres, J., 2006. Flushing submarine canyons. *Nature*, *444*(7117), pp.354-357.

6. Clarke, K.R., 1993. Non-parametric multivariate analyses of changes in community structure. *Australian journal of ecology*, *18*(1), pp.117-143.

7. Cronan, D.S., Rothwell, G. and Croudace, I., 2010. An ITRAX geochemical study of ferromanganiferous sediments from the Penrhyn Basin, South Pacific Ocean. *Marine Georesources and Geotechnology*, *28*(3), pp.207-221.

8. Danovaro, R., 2009. *Methods for the study of deep-sea sediments, their functioning and biodiversity*. CRC press.

9. Danovaro, R., Aguzzi, J., Fanelli, E., Billett, D., Gjerde, K., Jamieson, A., Ramirez-Llodra, E., Smith, C.R., Snelgrove, P.V.R., Thomsen, L. and Dover, C.V., 2017. An ecosystem-based deep-ocean strategy. *Science*, *355*(6324), pp.452-454.

10. Danovaro, R., Gambi, C., Dell'Anno, A., Corinaldesi, C., Fraschetti, S., Vanreusel, A., Vincx, M. and Gooday, A.J., 2008. Exponential decline of deep-sea ecosystem functioning linked to benthic biodiversity loss. *Current Biology*, *18*(1), pp.1-8.

11. Danovaro, R., Molari, M., Corinaldesi, C. and Dell'Anno, A., 2016. Macroecological drivers of archaea and bacteria in benthic deep-sea ecosystems. *Science Advances*, *2*(4), p.e1500961.

12. Danovaro, R., Snelgrove, P.V. and Tyler, P., 2014. Challenging the paradigms of deep-sea ecology. *Trends in ecology & evolution*, *29*(8), pp.465-475.

13. Dell'Anno, A., Corinaldesi, C., Magagnini, M. and Danovaro, R., 2009. Determination of viral production in aquatic sediments using the dilution-based approach. *Nature protocols*, *4*(7), pp.1013-1022.

14. DuBois, M., Gilles, K.A., Hamilton, J.K., Rebers, P.T. and Smith, F., 1956. Colorimetric method for determination of sugars and related substances. *Analytical chemistry*, *28*(3), pp.350-356.

15. Fiordelmondo, C., Manini, E., Gambi, C. and Pusceddu, A., 2003. Short-term impact of clam harvesting on sediment chemistry, benthic microbes and meiofauna in the Goro lagoon (Italy). *Chemistry and Ecology*, *19*(2-3), pp.173-187.

16. Gage, J.D. and Tyler, P.A., 1991. *Deep-sea biology: a natural history of organisms at the deep-sea floor*. Cambridge University Press.

17. Gerchakov, S.M. and Hatcher, P.G., 1972. Improved technique for analysis of carbohydrates in sediments 1. *Limnology and Oceanography*, *17*(6), pp.938-943.

18. Gillard, B., Purkiani, K., Chatzievangelou, D., Vink, A., Iversen, M.H. and Thomsen, L., 2019. Physical and hydrodynamic properties of deep sea mining-generated, abyssal sediment plumes in the Clarion Clipperton Fracture Zone (eastern-central Pacific). *Elementa: Science of the Anthropocene*, *7*.

19. Glover, A.G. and Smith, C.R., 2003. The deep-sea floor ecosystem: current status and prospects of anthropogenic change by the year 2025. *Environmental Conservation*, *30*(3), pp.219-241.

20. Gollner, S., Haeckel, M., Janssen, F., Lefaible, N., Molari, M., Papadopoulou, S., Reichart, G.J., Trabucho Alexandre, J., Vink, A. and Vanreusel, A., 2022. Restoration experiments in polymetallic nodule areas. *Integrated Environmental Assessment and Management*, *18*(3), pp.682-696.

21. Gollner, S., Kaiser, S., Menzel, L., Jones, D.O., Brown, A., Mestre, N.C., Van Oevelen, D., Menot, L., Colaço, A., Canals, M. and

Cuvelier, D., 2017. Resilience of benthic deep-sea fauna to mining activities. *Marine Environmental Research*, *129*, pp.76-101.

22. Grupe, B., Becker, H.J. and Oebius, H.U., 2001. Geotechnical and sedimentological investigations of deep-sea sediments from a manganese nodule field of the Peru Basin. *Deep Sea Research Part II: Topical Studies in Oceanography*, *48*(17-18), pp.3593-3608.

23. Halbach, P., Friedrich, G. and von Stackelberg, U. eds., 1988. *The manganese nodule belt of the Pacific Ocean: geological environment, nodule formation, and mining aspects* (p. 254). F. Enke.

24. Hein, J.R., Koschinsky, A. and Kuhn, T., 2020. Deep-ocean polymetallic nodules as a resource for critical materials. *Nature Reviews Earth & Environment*, *1*(3), pp.158-169.

25. Hein, J.R., Mizell, K., Koschinsky, A. and Conrad, T.A., 2013. Deep-ocean mineral deposits as a source of critical metals for high-and green-technology applications: Comparison with land-based resources. *Ore Geology Reviews*, *51*, pp.1-14.

26. Jones, D.O., Kaiser, S., Sweetman, A.K., Smith, C.R., Menot, L., Vink, A., Trueblood, D., Greinert, J., Billett, D.S., Arbizu, P.M. and Radziejewska, T., 2017. Biological responses to disturbance from simulated deep-sea polymetallic nodule mining. *PLoS One*, *12*(2), p.e0171750.

27. Khripounoff, A., Caprais, J.C., Crassous, P. and Etoubleau, J., 2006. Geochemical and biological recovery of the disturbed seafloor in polymetallic nodule fields of the Clipperton-Clarion Fracture Zone (CCFZ) at 5,000-m depth. *Limnology and Oceanography*, *51*(5), pp.2033-2041.

28. König, I., Haeckel, M., Lougear, A., Suess, E. and Trautwein, A.X., 2001. A geochemical model of the Peru Basin deep-sea floor—and the

response of the system to technical impacts. *Deep Sea Research Part II: Topical Studies in Oceanography*, *48*(17-18), pp.3737-3756.

29. Koschinsky, A. and Hein, J.R., 2003. Uptake of elements from seawater by ferromanganese crusts: solid-phase associations and seawater speciation. *Marine Geology*, *198*(3-4), pp.331-351.

30. Kuhn, T., Wegorzewski, A., Rühlemann, C. and Vink, A., 2017. Composition, formation, and occurrence of polymetallic nodules. *Deep-sea mining: Resource potential, technical and environmental considerations*, pp.23-63.

31. Lahti, L., Shetty, S., Blake, T. and Salojarvi, J., 2017. Tools for microbiome analysis in R. *Version*, *1*(5), p.28.

32. Leal Filho, W., Abubakar, I.R., Nunes, C., Platje, J., Ozuyar, P.G., Will, M., Nagy, G.J., Al-Amin, A.Q., Hunt, J.D. and Li, C., 2021. Deep seabed mining: A note on some potentials and risks to the sustainable mineral extraction from the oceans. *Journal of Marine Science and Engineering*, *9*(5), p.521.

33. Lutz, M.J., Caldeira, K., Dunbar, R.B. and Behrenfeld, M.J., 2007. Seasonal rhythms of net primary production and particulate organic carbon flux to depth describe the efficiency of biological pump in the global ocean. *Journal of Geophysical Research: Oceans*, *112*(C10).

34. MacIntyre, H.L., Geider, R.J. and Miller, D.C., 1996. Microphytobenthos: the ecological role of the "secret garden" of unvegetated, shallow-water marine habitats. I. Distribution, abundance and primary production. *Estuaries*, *19*, pp.186-201.

35. Marsh, J.B. and Weinstein, D.B., 1966. Simple charring method for determination of lipids. *Journal of lipid research*, *7*(4), pp.574-576.

36. McMurdie, P.J. and Holmes, S., 2013. phyloseq: an R package for reproducible interactive analysis and graphics of microbiome census data. *PloS one*, *8*(4), p.e61217.

37. Molari, M., Manini, E. and Dell'Anno, A., 2013. Dark inorganic carbon fixation sustains the functioning of benthic deep-sea ecosystems. *Global Biogeochemical Cycles*, *27*(1), pp.212-221.

38. Montagna, P.A., Coull, B.C., Herring, T.L. and Dudley, B.W., 1983. The relationship between abundances of meiofauna and their suspected microbial food (diatoms and bacteria). *Estuarine, Coastal and Shelf Science*, *17*(4), pp.381-394.

39. Oebius, H.U., Becker, H.J., Rolinski, S. and Jankowski, J.A., 2001. Parametrization and evaluation of marine environmental impacts produced by deep-sea manganese nodule mining. *Deep Sea Research Part II: Topical Studies in Oceanography*, *48*(17-18), pp.3453-3467.

40. Paul, S.A., Gaye, B., Haeckel, M., Kasten, S. and Koschinsky, A., 2018. Biogeochemical regeneration of a nodule mining disturbance site: trace metals, DOC and amino acids in deep-sea sediments and pore waters. *Frontiers in Marine Science*, *5*, p.117.

41. Plante, R., Plante-Cuny, M.R. and Reys, J.P., 1986. Photosynthetic pigments of sandy sediments on the north Mediterranean coast: their spatial distribution and its effect on sampling strategies. *Marine Ecology Progress Series*, pp.133-141.

42. Purser, A., Marcon, Y., Hoving, H.J.T., Vecchione, M., Piatkowski, U., Eason, D., Bluhm, H. and Boetius, A., 2016. Association of deep-sea incirrate octopods with manganese crusts and nodule fields in the Pacific Ocean. *Current Biology*, *26*(24), pp.R1268-R1269.

43. Pusceddu, A., Bianchelli, S., Martín, J., Puig, P., Palanques, A., Masqué, P. and Danovaro, R., 2014. Chronic and intensive bottom

trawling impairs deep-sea biodiversity and ecosystem functioning. *Proceedings of the National Academy of Sciences*, *111*(24), pp.8861-8866.

44. Quast, C., Pruesse, E., Yilmaz, P., Gerken, J., Schweer, T., Yarza, P., Peplies, J. and Glöckner, F.O., 2012. The SILVA ribosomal RNA gene database project: improved data processing and web-based tools. *Nucleic acids research*, *41*(D1), pp.D590-D596.

45. Radziejewska, T., 2002. Responses of deep-sea meiobenthic communities to sediment disturbance simulating effects of polymetallic nodule mining. *International Review of Hydrobiology: A Journal Covering all Aspects of Limnology and Marine Biology*, *87*(4), pp.457-477.

46. Ramirez-Llodra, E., Tyler, P.A., Baker, M.C., Bergstad, O.A., Clark, M.R., Escobar, E., Levin, L.A., Menot, L., Rowden, A.A., Smith, C.R. and Van Dover, C.L., 2011. Man and the last great wilderness: human impact on the deep sea. *PLoS one*, *6*(8), p.e22588.

47. Rastelli, E., Dell'Anno, A., Corinaldesi, C., Middelboe, M., Noble, R.T. and Danovaro, R., 2016. Quantification of viral and prokaryotic production rates in benthic ecosystems: A methods comparison. *Frontiers in Microbiology*, *7*, p.1501.

48. Smith, C.R., Levin, L.A., Koslow, A., Tyler, P.A. and Glover, A.G., 2008. The near future of the deep seafloor ecosystems, in: Polunin, N.V. ed., 2008. *Aquatic ecosystems: trends and global prospects*. Cambridge University Press.

49. Snelgrove, P.V., 1997. The importance of marine sediment biodiversity in ecosystem processes. *Ambio*, pp.578-583.

50. Stoeck, T., Bass, D., Nebel, M., Christen, R., Jones, M.D., BREINER, H.W. and Richards, T.A., 2010. Multiple marker parallel tag environmental DNA sequencing reveals a highly complex eukaryotic community in marine anoxic water. *Molecular ecology*, *19*, pp.21-31.

51. Stratmann, T., Lins, L., Purser, A., Marcon, Y., Rodrigues, C.F., Ravara, A., Cunha, M.R., Simon-Lledó, E., Jones, D.O., Sweetman, A.K. and Köser, K., 2018. Abyssal plain faunal carbon flows remain depressed 26 years after a simulated deep-sea mining disturbance. *Biogeosciences*, *15*(13), pp.4131-4145.

52. Stratmann, T., Soetaert, K., Kersken, D. and van Oevelen, D., 2021. Polymetallic nodules are essential for food-web integrity of a prospective deep-seabed mining area in Pacific abyssal plains. *Scientific Reports*, *11*(1), p.12238.

53. Thiel, H. and Tiefsee-Umweltschutz, F., 2001. Evaluation of the environmental consequences of polymetallic nodule mining based on the results of the TUSCH Research Association. *Deep Sea Research Part II: Topical Studies in Oceanography*, *48*(17-18), pp.3433-3452.

54. Thurber, A.R., Sweetman, A.K., Narayanaswamy, B.E., Jones, D.O., Ingels, J. and Hansman, R.L., 2014. Ecosystem function and services provided by the deep sea. *Biogeosciences*, *11*(14), pp.3941-3963.

55. United Nations. Division for Ocean Affairs, the Law of the Sea, United Nations. Office of Legal Affairs and International Seabed Authority, 2004. *Marine Mineral Resources: Scientific Advances and Economic Perspectives*. United Nations Publications.

56. Van Dover, C.L., Ardron, J.A., Escobar, E., Gianni, M., Gjerde, K.M., Jaeckel, A., Jones, D.O.B., Levin, L.A., Niner, H.J., Pendleton, L. and Smith, C.R., 2017. Biodiversity loss from deep-sea mining. *Nature Geoscience*, *10*(7), pp.464-465.

57. Vanreusel, A., Hilario, A., Ribeiro, P.A., Menot, L. and Arbizu, P.M., 2016. Threatened by mining, polymetallic nodules are required to preserve abyssal epifauna. *Scientific reports*, *6*(1), pp.1-6.

58. Volz, J.B., Haffert, L., Haeckel, M., Koschinsky, A. and Kasten, S., 2020. Impact of small-scale disturbances on geochemical conditions, biogeochemical processes and element fluxes in surface sediments of the eastern Clarion–Clipperton Zone, Pacific Ocean. *Biogeosciences*, *17*(4), pp.1113-1131.

59. Von Stackelberg, U., 2017. Manganese nodules of the Peru Basin. In *Handbook of marine mineral deposits* (pp. 197-238). Routledge.

60. Vonnahme, T.R., Molari, M., Janssen, F., Wenzhöfer, F., Haeckel, M., Titschack, J. and Boetius, A., 2020. Effects of a deep-sea mining experiment on seafloor microbial communities and functions after 26 years. *Science Advances*, *6*(18), p.eaaz5922.

61. Yilmaz, P., Parfrey, L.W., Yarza, P., Gerken, J., Pruesse, E., Quast, C., Schweer, T., Peplies, J., Ludwig, W. and Glöckner, F.O., 2014. The SILVA and "all-species living tree project (LTP)" taxonomic frameworks. *Nucleic acids research*, *42*(D1), pp.D643-D648.